Phycologia (2008) Volume 47 (4), 371–391 Published 3 July 2008

Pseudostriatella (Bacillariophyta): a description of a new araphid diatom genus based on observations of frustule and auxospore structure and 18S rDNA phylogeny

SHINYA SATO[1]*, DAVID G. MANN[2], SATOKO MATSUMOTO[3] AND LINDA K. MEDLIN[1]

[1]*Alfred Wegener Institute for Polar and Marine Research, Am Handelshafen 12, D-27570 Bremerhaven, Germany*
[2]*Royal Botanic Garden, Edinburgh EH3 5LR, Scotland, United Kingdom*
[3]*Choshi Fisheries High School, 1-1-12 Nagatsuka Cho, Choshi City, Chiba, Japan*

S. SATO, D.G. MANN, S. MATSUMOTO AND L.K. MEDLIN. 2008. *Pseudostriatella* (Bacillariophyta): a description of a new araphid diatom genus based on observations of frustule and auxospore structure and 18S rDNA phylogeny. *Phycologia* 47: 371–391. DOI: 10.2216/08-02.1

Pseudostriatella oceanica gen et. sp. nov. is a marine benthic diatom that resembles *Striatella unipunctata* in gross morphology, attachment to the substratum by a mucilaginous stalk and possession of septate girdle bands. In light microscopy, *P. oceanica* can be distinguished from *S. unipunctata* by plastid shape, absence of truncation of the corners of the frustule, indiscernible striation and absence of polar rimoportulae. With scanning electron microscopy, *P. oceanica* can be distinguished by a prominent but unthickened longitudinal hyaline area, pegged areolae, multiple marginal rimoportulae and perforated septum. The hyaline area differs from the sterna of most pennate diatoms in being porous toward its expanded ends; in this respect, it resembles the elongate annuli of some centric diatoms, such as *Attheya* and *Odontella*. 18S rDNA phylogeny places *P. oceanica* among the pennate diatoms and supports a close relationship between *P. oceanica* and *S. unipunctata*, but the genetic distance between them, coupled with the morphological differences, justifies separation at genus level. However, the affinity of the *P. oceanica* – *S. unipunctata* clade remains unresolved both in molecular and in morphological study. Both genera are only distantly related to *Hyalosira* and *Grammatophora*, despite similarities in frustule structure and growth habit, arguing against their inclusion in the same family. The auxospore is covered with series of transverse and longitudinal bands, but the structure and arrangement of these bands appear to be more similar to the properizonia of some centric diatoms than to the classic type of perizonium seen in other pennate diatoms; a few scales are also present. The differences between properizonia and perizonia are discussed.

KEY WORDS: 18S rDNA, Araphid diatom, Auxospore, Evolution, Fine structure, Morphology, Perizonium, Phylogeny, *Pseudostriatella oceanica*, *Striatella*, Taxonomy

INTRODUCTION

Benthic diatoms are ubiquitous in shallow coastal environments and are one of the most taxonomically diverse groups of organisms in estuarine ecosystems (Sullivan & Currin 2000). Because of their high primary production rates, benthic diatoms play an important role in the functioning of benthic trophic webs in intertidal mudflats and shallow-water ecosystems of temperate to tropical regions (Cahoon 1999; Underwood & Kromkamp 1999). Araphid pennate diatoms (diatoms with a sternum but lacking a raphe system; see *Terminology*) are important components of these coastal assemblages, particularly among communities attached to macrophytes and macroalgae, animals, rocks and sand grains (Round *et al.* 1990). Taxonomically, araphid diatoms have long been neglected, perhaps because of their morphological simplicity; according to Round *et al.* (1990), 'in many ways the classification of the araphid group is the most difficult because unlike the centric series their valve structure is rather simple, and unlike the raphid series, the plastids and their arrangements have few distinguishing features'. Thus, in spite of their high abundance, the defining features of the main groups of araphid diatoms are not fully established.

To obtain a more complete picture of the natural history of araphid diatoms, we have been collecting samples worldwide from coastal regions. Recently we encountered a new diatom that superficially resembled *Striatella unipunctata* (Lyngbye) Agardh. Scanning electron microscopy (SEM) revealed, however, that this diatom differed from *S. unipunctata* in several features that are generally used as taxonomic characters among araphid diatoms, including characteristics of the sternum, striae, areolae, apical pore field, rimoportula and septum. Given these observations, together with information on the plastids and 18S rDNA sequences, we conclude that the diatom should be described as a new genus, *Pseudostriatella*.

We have also been able to make detailed observations on the fine structure of auxospores produced spontaneously in monoclonal cultures. With the advent of electron microscopy, particularly SEM, information about auxospore structure has greatly increased (e.g. Crawford 1974; Mann 1982b; von Stosch 1982; Cohn *et al.* 1989; Kaczmarska *et al.* 2000, 2001; Kobayashi *et al.* 2001; Schmid & Crawford 2001; Nagumo 2003; Sato *et al.* 2004, 2008a, b; Amato *et al.* 2005; Tiffany 2005; Toyoda *et al.* 2005, 2006; Trobajo *et al.*

* Corresponding author (shinya.sato@awi.de).

2006; Poulíčková & Mann 2006; Poulíčková *et al.* 2007). However, although it has become clear that some aspects of the fine structure of auxospores have phylogenetic significance (e.g. Medlin & Kazcmarska 2004), there is still insufficient information to reveal how the structure and development of auxospores have evolved in the major diatom groups, especially among the lineages of araphid pennate diatoms. Indeed, the only detailed information available concerning araphid pennates is the account of *Rhabdonema* Kützing by von Stosch (1962, 1982) and the SEM studies of *Gephyria media* Arnott (Sato *et al.* 2004), *Grammatophora marina* (Lyngbye) Kützing (Sato *et al.* 2008a) and *Tabularia parva* (Kützing) Williams & Round (Sato *et al.* 2008b). In the present study, we compare the auxospore fine structure in these diatoms with that of *Pseudostriatella oceanica* and discuss the evolutionary relationships of *Pseudostriatella*.

MATERIAL AND METHODS

Collections and cultures

Both natural specimens and clonal cultures were examined in this study. Vegetative cells of the *P. oceanica* examined here were collected by S. Matsumoto at Yumigahama Beach, Minamiizu, Shizuoka Prefecture, Japan, on 20 May 2005, attached to *Cladophora* sp., and by B.K. Petkus at Horseneck State Beach, Westport, Massachusetts, USA, on August 2006, from bottom sand. For morphological comparison, *S. unipunctata*, the generitype of the genus *Striatella*, was collected by L.K. Medlin from Banyuls sur Mer, France, on 13 February 2005. Single cells were isolated from the American and French samples to obtain clonal cultures. Cultures were maintained in IMR medium (Eppley *et al.* 1967) at 15°C under cool-white fluorescent light on a 14 : 10-h (L : D) photoperiod at a photon flux density of 30–40 μmol photons m^{-2} s^{-1}. A coverslip was placed on the bottom of the culture vessel to be colonized with cells producing auxospores. Both strains examined in this study, *P. oceanica* s0384 and *S. unipunctata* s0208, are currently available on request to the first author but may not survive long-term in culture (*cf.* Chepurnov *et al.* 2004).

Microscopy

An Axioplan (Zeiss) light microscope (LM) with bright field, differential interference contrast (DIC) or phase contrast optics was used to observe living cells and cleaned frustules. To photograph live specimens attached to the bottom of the culture vessel, a Zeiss Axiovert 35 inverted microscope was used, equipped with an AxioCam MRc digital camera. To remove organic material from the frustule, samples were treated as follows (modified from Nagumo & Kobayashi 1990): (1) the sample was centrifuged to make a pellet and the supernatant discarded; (2) the pellet was resuspended in distilled water, and steps 1 and 2 were then repeated several times to remove salts; (3) to remove organic matter, the pellet was suspended (using a vortex mixer) in an equal volume of Drano Power-Gel (Johnson Wax), a strong domestic drain cleaner; (4) the suspension was left at room temperature for *c.* 30 min; and (5) steps 1 and 2 were repeated several times to remove decomposition products. Cleaned frustules were then mounted in Mount-media (refractive index n20/D = 1.50; Wako).

For SEM examination, cleaned material was air-dried onto coverslips. To observe auxospores, coverslips to which the auxospore mother cells had already become attached were immersed in 10% glutaraldehyde for 1 h at room temperature, then washed with distilled water, air-dried and fixed to SEM stubs with carbon tape. For observations of cells still attached to the substratum by mucilaginous stalks, host plants were fixed with 10% glutaraldehyde for 2 h at 4°C, rinsed with distilled water several times to remove the glutaraldehyde, dehydrated using increasing concentrations of t-butyl alcohol and freeze-dried using a JFD-310 instrument (JEOL). Freeze-dried specimens were attached to the stub directly with carbon tape. All SEM specimens were coated with gold using an SC 500 sputter coater (Emscope). A QUANTA 200F (FEI) was used for SEM observation at an accelerating voltage of 3–10 kV and *c.* 10 mm working distance. All the images included in this paper are from cultured strains, except for those from freeze-dried material (Figs 9–13). Captured images were adjusted with Adobe Photoshop.

DNA methods

Samples of *c.* 500 ml of culture were filtered through 3-μm-pore-diameter membrane filters (Millipore). Filters were immersed in 500 μl DNA extraction buffer containing 2% (w/v) CTAB, 1.4 M NaCl, 20 mM EDTA, 100 mM Tris-HCl, pH 8, 0.2% (w/v) PVP, 0.01% (w/v) SDS and 0.2% β-mercaptoethanol. Immersed filters were incubated at 65°C for 5 min, vortexed for a few seconds and then discarded. Subsequently, the buffer was cooled briefly on ice. DNA was extracted with an equal volume of chloroform–isoamyl alcohol (24 : 1 [v/v]) and centrifuged in a tabletop Eppendorf microfuge (Eppendorf) at maximum speed (14,000 rpm) for 10 min. The aqueous phase was collected, re-extracted with chloroform–isoamyl alcohol and centrifuged as described previously. Next, the aqueous phase was mixed thoroughly with 0.8 volumes of ice-cold 100% isopropanol, left on ice for 5 min and subsequently centrifuged in a precooled Eppendorf microfuge at maximum speed for 15 min. DNA pellets were washed in 500 μl 70% (v/v) ethanol, centrifuged for 6 min and then allowed to air-dry after decanting off the ethanol. DNA pellets were dissolved overnight in 100 μl water. The quantity and quality of DNA were examined by agarose gel electrophoresis against known standards.

The targeted marker sequence comprised the 18S rDNA within the nuclear rDNA cistron. The marker was PCR-amplified in 25-μl volumes containing 10 ng DNA, 1 mM dNTPs, 0.5 μM of forward primer, 0.5 μM of reverse primer, 1× Roche diagnostics PCR reaction buffer (Roche Diagnostics) and 1 unit *Taq* DNA polymerase (Roche). The PCR cycling comprised an initial 4-min heating step at 94°C, followed by 35 cycles of 94°C for 2 min, 56°C for 4 min and 72°C for 2 min and a final extension at 72°C for 10 min. PCR products were generated using the forward primer A and a reverse primer B (Medlin *et al.* 1988)

without the polylinkers. The quantity and length of products were examined by agarose gel electrophoresis against known standards. Excess primers and dNTPs were removed from PCR product using the QIAQuick purification kit (QIAGEN), following the manufacturer's instructions. The cleaned PCR products were then electrophoresed on an ABI 3100 Avant sequencer (Applied Biosystems) using Big Dye Terminator v. 3.1 sequencing chemistry (Applied Biosystems) with the sequencing primers specified by Elwood *et al.* (1985).

Data analyses

The obtained 18S rDNA sequences were aligned with publicly available sequences retrieved from GenBank (Table 1), first using ClustalX (Thompson *et al.* 1997) and then refined by referring to the secondary structure model of the 18S rRNA at the database of the structure of rRNA (Van de Peer *et al.* 1998). There is extreme length variation in some rRNAs (e.g. Gillespie *et al.* 2005), and replication slippage often leads to convergence on similar primary and secondary structures (Hancock & Vogler 2000; Shull *et al.* 2001). Homology assessment in such regions was difficult or impossible, so that the highly variable regions (most peripheral regions of the 18S rRNA secondary structure) were removed from the alignment using BioEdit 7.0.2 (Hall 1999) by referring to the variability map of *Saccharomyces cerevisiae* (Van de Peer *et al.* 1993), resulting in 1713 nucleotides in the data set.

The data set consisted of 181 OTUs including the closest relatives of the diatoms *Bolidomonas mediterranea* Guillou & Chrétiennot-Dinet and *B. pacifica* Guillou & Chrétiennot-Dinet (Guillou *et al.* 1999) as outgroups. The alignment examined in this study is available at TreeBASE (SN3793).

To determine which model of sequence evolution best fits the data, hierarchical likelihood ratio tests and the Akaike information criterion were performed using Modeltest 3.7 (Posada & Crandall 1998), and both tests selected the GTR + I + G model. This model had the following parameters: base frequencies = A: 0.2685, C: 0.1643, G: 0.2539 and T: 0.3133; substitution rates were A–C = 1.2232, A–G = 3.1535, A–T = 1.2675, C–G = 1.4955, C–T = 5.5072 and G–T = 1.0000; the proportion of invariant sites was 0.2825; and among-site rate heterogeneity was described by a gamma distribution with a shape parameter of 0.6058. Phylogenies were reconstructed with PAUP v. 4.0b10 (Swofford 2002) using neighbour joining (NJ) of likewise-constrained pairwise maximum likelihood (ML) distances. Nodal support was estimated using NJ bootstrap analyses using the same settings (1000 replicates).

Maximum parsimony (MP) tree searches were done with the 'new technology' search algorithm implemented in the Willi Hennig Society edition of TNT 1.1 (http://www.zmuc.dk/public/phylogeny/TNT). One hundred random addition sequence replicates were performed with default values. Nonparametric bootstrap analyses were done 1000 times with the 'traditional' search algorithm in TNT.

Maximum likeli hood analyses were performed by RAxML-VI-HPC, v. 2.2.3 (Stamatakis *et al.* 2005) with the GTRMIX model. The analyses were performed 100 times to find the best topology receiving the best likelihood using different random starting MP trees (one round of taxon addition) and the rapid hill-climbing algorithm (i.e. option -f d in RAxML). Bootstrap values were obtained by 100 replications with the GTRCAT model.

The Message Passing Interface (MPI) version of MrBayes 3.1.2 (Huelsenbeck & Ronquist 2001; Ronquist & Huelsenbeck 2003; Altekar *et al.* 2004) was used for Bayesian analyses with the GTR + I + G model to estimate the posterior probability distribution using Metropolis-Coupled Markov chain Monte Carlo (MCMCMC) (Ronquist & Huelsenbeck 2003). The MCMCMC from a random starting tree was used in this analysis with two independent runs and one cold and three heated chains. The Bayesian analyses were run for 20 million generations each with trees sampled every 100th generation. To increase the probability of chain convergence, we sampled trees after the standard deviation values of the two runs dipped below 0.01 to calculate the posterior probabilities (i.e. after 8,300,000 generations). The remaining phylogenies were discarded as burn-in.

Terminology

Terminology follows Anonymous (1975) and (particularly for auxospore structures) Round et al. (1990). Molecular phylogenetic studies of diatoms have revealed that historical diatom classifications do not reflect a natural system and that araphid pennate diatoms are paraphyletic in most gene phylogenies, for example, using nuclear 18S ribosomal DNA (rDNA) and plastid 16S rDNA (Medlin & Kaczmarska 2004). Nevertheless, we use the terms *araphid* and *centric* here because they refer to key morphological features or their absence. In this paper, the term *araphid pennate diatom* follows the traditional definition, that is, a diatom that has an elongate valve with a central or slightly lateral sternum, apical pore fields and often also apical rimoportulae but that lacks a raphe slit. We do not imply that this corresponds to a mono- (holo-) phyletic group or that it should be accorded any taxonomic status.

RESULTS

Pseudostriatella S. Sato, Mann & Medlin *gen. nov.*

Figs 1–53

Cellulae rectangulares in aspectu cincturae angulis rotundatis, angulo unico per stipitem muci ad substratum adhaerentes. Chloroplasti c. *10 dispersi et cellulam complentes. Taeniae cincturae numerosae apertae septo conspicuo poros aliquot praebenti. Valvae lanceolatae, ocello ad utrumque polum, fronte in sectione transversali arcuata, sine limbo distincto. Striae irregulares in LM non manifestae. Sternum typicum nullum sed area hyalina secus axem longam adest. Areolae per clavulas occlusae, igitur aperturis dendriticis instructae. Rimoportulae multae dispersae, forma interna variabili.*

Cells attached to the substratum by a mucilage stalk at one corner of the frustule, rectangular in girdle view, with rounded corners. Plastids *c.* 10 per cell, scattered and filling the cell. Copulae numerous open hoops, each with a conspicuous septum containing several pores. Valve lanceolate, with an apical pore field (ocellus) at each pole. Valve face arched, without a distinct mantle. Striae irregular, unresolved with LM. Sternum apparently absent, but a

Table 1. List of taxon and GenBank accession numbers for 18S rDNA sequences used in this study.

Taxon	Accession no.
Aulacoseira ambigua (Grunow) Simonsen	X85404
Aulacoseira baicalensis (Meyer) Simonsen	AJ535185
Aulacoseira baicalensis (Meyer) Simonsen	AJ535186
Aulacoseira baicalensis (Meyer) Simonsen	AY121821
Aulacoseira distans (Ehrenberg) Simonsen	X85403
Aulacoseira islandica (Müller) Simonsen	AJ535183
Aulacoseira islandica (Müller) Simonsen	AY121820
Aulacoseira nyassensis (Müller) Simonsen	AJ535187
Aulacoseira nyassensis (Müller) Simonsen	AY121819
Aulacoseira skvortzowii Edlund, Stoermer *et* Taylor	AJ535184
Aulacoseira subarctica (Müller) Haworth	AY121818
Actinocyclus curvatulus Janisch	X85401
Actinoptychus seniarius (Ehrenberg) Héribaud	AJ535182
Bellerochea malleus (Brightwell) van Heurck	AF525671
Biddulphiopsis titiana (Grunow) von Stosch *et* Simonsen	AF525669
Chaetoceros curvisetus Cleve	AY229895
Chaetoceros debilis Cleve	AY229896
Chaetoceros didymus Ehrenberg	X85392
Chaetoceros gracilis Schütt	AY229897
Chaetoceros rostratus Lauder	X85391
Chaetoceros sp.	AF145226
Chaetoceros sp.	AJ535167
Chaetoceros sp.	X85390
Corethron criophilum Castracane	X85400
Corethron inerme Karsten	AJ535180
Corethron hystrix Hensen	AJ535179
Coscinodiscus radiatus Ehrenberg	X77705
Cyclotella meneghiniana Kützing	AJ535172
Cyclotella meneghiniana Kützing	AY496206
Cyclotella meneghiniana Kützing	AY496207
Cyclotella meneghiniana Kützing	AY496210
Cyclotella meneghiniana Kützing	AY496212
Cyclotella cf. *scaldensis*	AY496208
Cymatosira belgica Grunow	X85387
Detonula confervacea (Cleve) Gran	AF525672
Ditylum brightwellii (West) Grunow in Van Heurck	AY188181
Ditylum brightwellii (West) Grunow in Van Heurck	AY188182
Ditylum brightwellii (West) Grunow in Van Heurck	X85386
Eucampia antarctica (Castracane) Mangin	X85389
Guinardia delicatula (Cleve) Hasle	AJ535192
Guinardia flaccida (Castracane) H. Peragallo	AJ535191
Helicotheca tamesis (Schrubsole) Ricard	X85385
Lampriscus kittonii Schmidt	AF525667
Lauderia borealis Cleve	X85399
Leptocylindrus danicus Cleve	AJ535175
Leptocylindrus minimus Gran	AJ535176
Lithodesmium undulatum Ehrenberg	Y10569
Melosira varians Agardh	AJ243065
Melosira varians Agardh	X85402
Odontella sinensis (Greville) Grunow	Y10570
Papiliocellulus elegans Hasle, von Stosch *et* Syvertsen	X85388
Paralia sol (Ehrenberg) Crawford	AJ535174
Planktoniella sol (Wallich) Schütt	AJ535173
Pleurosira laevis (Ehrenberg) Comperé	AF525670
Porosira pseudodenticulata (Hustedt) Jousé	X85398
Proboscia alata (Brightwell) Sundström	AJ535181
Rhizosolenia imbricate Brightwell	AJ535178
Rhizosolenia similoides Cleve-Euler	J535177
Rhizosolenia setigera Brightwell	M87329
Skeletonema costatum (Greville) Cleve	X52006
Skeletonema costatum (Greville) Cleve	X85395
Skeletonema menzelii Guillard, Carpenter *et* Reimer	AJ535168
Skeletonema menzelii Guillard, Carpenter *et* Reimer	AJ536450
Skeletonema pseudocostatum Medlin	AF462060
Skeletonema pseudocostatum Medlin	X85393
Skeletonema subsalsum (Cleve-Euler) Bethge	AJ535166
Skeletonema sp.	AJ535165

Table 1. Continued

Taxon	Accession no.
Stephanopyxis cf. *broschii*	M87330
Thalassiosira eccentrica (Ehrenberg) Cleve	X85396
Thalassiosira guillardii Hasle	AF374478
Thalassiosira oceanica Hasle	AF374479
Thalassiosira pseudonana Hasle *et* Heimdal	AJ535169
Thalassiosira pseudonana Hasle *et* Heimdal	AF374481
Thalassiosira rotula Meunier	AF374480
Thalassiosira rotula Meunier	AF462058
Thalassiosira rotula Meunier	AF462059
Thalassiosira rotula Meunier	X85397
Thalassiosira weissflogii (Grunow) Fryxell *et* Hasle	AF374477
Thalassiosira weissflogii (Grunow) Fryxell *et* Hasle	AJ535170
Thalassiosira sp.	AJ535171
Toxarium undulatum Bailey	AF525668
Asterionella formosa Hassall	AF525657
Asterionellopsis glacialis (Castracane) Round	X77701
Asterionellopsis glacialis (Castracane) Round	AY216904
Asteroplanus karianus[1] (Grunow in Cleve *et* Grunow) Gardner et Crawford	Y10568
Cyclophora tenuis Castracane	AJ535142
Diatoma hyemalis (Roth) Heiberg	AB085829
Diatoma tenue Agardh	AJ535143
Fragilaria crotonensis Kitton	AF525662
Fragilariforma virescens (Ralfs) Williams *et* Round	AJ535137
Grammatophora gibberula Kützing	AF525656
Grammatophora oceanica Ehrenberg	AF525655
Grammatophora marina (Lyngbye) Kützing	AY216906
Grammonema striatula Agardh[1]	X77704
Grammonema cf. *islandica*[1]	AJ535190
Grammonema sp.[1]	AJ535141
Hyalosira delicatula Kützing	AF525654
Licmophora juergensii Agardh	AF525661
Nanofrustulum shiloi (Lee, Reimer *et* McEnery) Round, Hallsteinsen et Paasche	AF525658
Pseudostriatella oceanica S. Sato, Mann *et* Medlin	AB379680
Rhabdonema arcuatum (Agardh) Kützing	AF525660
Rhaphoneis cf. *belgica* (Grunow in van Heurck) Grunow in van Heurck	X77703
Staurosira construens Ehrenberg	AF525659
Striatella unipunctata (Lyngbye) Agardh	AF525666
Synedra sp.[2]	AJ535138
Tabularia tabulata (Agardh) Williams *et* Round	AY216907
Talaroneis posidoniae Kooistra et De Stefano	AY216905
Thalassionema nitzschioides (Grunow) Hustedt	X77702
Thalassionema sp.	AJ535140
Synedra ulna Nitzsch	AJ535139
Achnanthes bongrainii (M. Peragallo) A. Mann	AJ535150
Achnanthes sp.	AJ535151
Amphora montana Krasske	AJ243061
Amphora cf. *capitellata*	AJ535158
Amphora cf. *proteus*	AJ535147
Anomoeoneis sphaerophora (Ehrenberg) Pfitzer	AJ535153
Bacillaria paxillifer (Müller) Hendey	M87325
Campylodiscus ralfsii Gregory	AJ535162
Cocconeis cf. *molesta*	AJ535148
Cylindrotheca closterium (Ehrenberg) Reimann *et* Lewin	M87326
Cymbella cymbiformis Agardh	AJ535156
Encyonema triangulatum Kützing	AJ535157
Entomoneis cf. *alata*	AJ535160
Eolimna minima (Grunow) Lange-Bertalot	AJ243063
Eolimna subminuscula (Manguin) Moser, Lange-Bertalot et Metzeltin	AJ243064
Eunotia formica var. *sumatrana* Hustedt	AB085830
Eunotia monodon var. *asiatica* Skvortzow	AB085831
Eunotia pectinalis (Dillwyn) Rabenhorst	AB085832
Eunotia cf. *pectinalis* f. *minor*	AJ535146
Eunotia sp.	AJ535145
Fragilariopsis sublineata Hasle	AF525665

Table 1. Continued

Taxon	Accession no.
Gomphonema parvulum Kützing	AJ243062
Gomphonema pseudoaugur Lange-Bertalot	AB085833
Lyrella atlantica (Schmidt) D. G. Mann	AJ544659
Navicula cryptocephala var. *veneta* (Kützing) Grunow	AJ297724
Navicula diserta Hustedt	AJ535159
Navicula pelliculosa (Brébisson *ex* Kützing) Hilse	AJ544657
Nitzschia apiculata (Gregory) Grunow	M87334
Nitzschia frustulum (Kützing) Grunow	AJ535164
Pinnularia cf. *interrupta*	AJ544658
Pinnularia sp.	AJ535154
Phaeodactylum tricornutum Bohlin	AJ269501
Planothidium lanceolatum (Brébisson *ex* Kützing) Round et Bukhtiyarova	AJ535189
Pleurosigma sp.	AF525664
Pseudogomphonema sp.	AF525663
Pseudogomphonema sp.	AJ535152
Pseudo-nitzschia multiseries (Hasle) Hasle	U18241
Pseudo-nitzschia pungens (Grunow *ex* Cleve) Hasle	U18240
Rossia sp.	AJ535144
Sellaphora capitata Mann *et* McDonald	AJ535155
Sellaphora pupula (Kützing) Mereschkowsky	AJ544645
Sellaphora pupula (Kützing) Mereschkowsky	AJ544651
Sellaphora pupula (Kützing) Mereschkowsky	AJ544647
Sellaphora pupula (Kützing) Mereschkowsky	AJ544648
Sellaphora pupula (Kützing) Mereschkowsky	AJ544649
Sellaphora pupula (Kützing) Mereschkowsky	AJ544650
Sellaphora pupula (Kützing) Mereschkowsky	AJ544652
Sellaphora pupula (Kützing) Mereschkowsky	AJ544653
Sellaphora pupula (Kützing) Mereschkowsky	AJ544654
Sellaphora laevissima (Kützing) D. G. Mann	AJ544655
Sellaphora laevissima (Kützing) D. G. Mann	AJ544656
Surirella fastuosa var. *cuneata* (Schmidt) H. Peragallo *et* M. Peragallo	AJ535161
Thalassiosira antarctica Comber	AF374482
Undatella sp.	AJ535163
Bolidomonas mediterranea Guillou *et* Chretéinnot-Dinet	AF123596
Bolidomonas pacifica Guillou *et* Chréteinnot-Dinet	AF123595
Bolidomonas pacifica Guillou *et* Chréteinnot-Dinet	AF167153
Bolidomonas pacifica Guillou *et* Chréteinnot-Dinet	AF167154
Bolidomonas pacifica Guillou *et* Chréteinnot-Dinet	AF167155
Bolidomonas pacifica Guillou *et* Chréteinnot-Dinet	AF167156
Bolidomonas pacifica Guillou *et* Chréteinnot-Dinet	AF167157
Convoluta convoluta diatom endosymbiont	AY345013
Peridinium foliaceum endosymbiont	Y10567
Peridinium balticum endosymbiont	Y10566
Uncultured diatom	AY180014
Uncultured diatom	AY180015
Uncultured diatom	AY180016
Uncultured diatom	AY180020
Uncultured eukaryote	AY082977
Uncultured eukaryote	AY082992
Uncultured marine diatom	AF290085

[1] Name change since deposit.
[2] Likely a new genus collected from a marine habitat (Medlin *et al.* 2008a).

hyaline area is present along the long axis. Areolae occluded by peg-like structures and therefore with dendritic apertures. Many rimoportulae present, of variable form internally.

TYPE SPECIES: ***P. oceanica* S. Sato, Mann & Medlin *sp. nov.***

Descriptio speciei eadem est ac descriptio generis; valvae 16.0–47.8 μm longae, 4.4–5.3 μm latae.

HOLOTYPE: BRM Zu6/38.

ISOTYPE: TNS-AL-53995.

TYPE LOCALITY: Horseneck State Beach, Westport, MA, USA.

DISTRIBUTION: Known only from the type locality and Yumigahama Beach, Minamiizu, Shizuoka Prefecture, Japan.

Morphology of vegetative cells

In the culture vessel, cells of *P. oceanica* attached to the bottom, usually by means of a mucilaginous stalk secreted from one corner, which reached a maximum length of *c.* 20 μm (Fig. 1). Cells occasionally attached to each other to make zigzag chains (not shown), but this was seen only in culture, and chains of over five cells were never found. About 10 lobed plastids were scattered through the cell (Fig. 2). A prominent body, likely a pyrenoid, was often visible at the centre of a plastid (Fig. 2, arrow). In girdle view, when the focus was on the surface of the cell, longitudinal rib-like thickenings were visible on some of the girdle bands (Fig. 3). Spots could sometimes be seen on the valve mantle (e.g. at arrow, Fig. 3), and tiny projections were sometimes visible extending inwards from the valve face (e.g. at the centre of the valve in Fig. 4); these features probably represent rimoportulae (see below).

The valves were lanceolate with acute ends (Figs 5, 6). No striae could be resolved in LM with bright field (Fig. 5), DIC (Fig. 6) or phase contrast optics (not shown). The valve length was 16.0–47.8 μm. Auxospore mother cells measured 16.9 ± 0.6 μm (mean ± *s*, $n = 8$), and initial cells were 41.1 ± 3.1 μm ($n = 12$). The valve width was 4.4–5.3 μm. Apical pore fields were recognisable in LM as hyaline areas at both ends of a valve (Figs 5, 6).

The frustule had numerous girdle bands (*c.* 10 per theca: Figs 8, 10), each being an incomplete hoop, open at one end (Fig. 7). The closed end of each band bore a septum, which extended inwards by one-sixth to one-eighth of the valve length (Figs 4, 7). The alternation of the septa (Figs 8, 12, 32) gave a *Striatella*-like appearance to the cell in girdle view (Fig. 3).

Observations of freeze-dried specimens from field material revealed that the surface of the host plant was covered with bacteria (Figs 9, 10, 13). The long mucilaginous stalk (Fig. 9) was secreted from one of the apical pore fields (Fig. 11), but no secretion occurred from other (Fig. 12). The thickness of the stalk was *c.* 1 μm (Figs 9, 10, 13). The surface of the mucilaginous stalk was not uniform but comprised many fine strings and thus appeared fibrous (Fig. 13).

The valve face was smoothly rounded (Fig. 14), lacking an abrupt change between it and the mantle. The areolae were irregularly scattered over some parts of the valve, especially towards the poles, but formed parallel striae towards the centre and radiating striae elsewhere (Fig. 14). A clearly defined sternum was absent, but there was an irregular hyaline area along the long axis of the valve (Fig. 14). This hyaline area (1) did not occupy the whole but at most only about one-half of the long axis of the valve (Fig. 14), (2) was wider at both ends than in the centre (Fig. 14), and (3) was perforated by small pores in the two wide end sections (Fig. 15). Apical pore fields were present

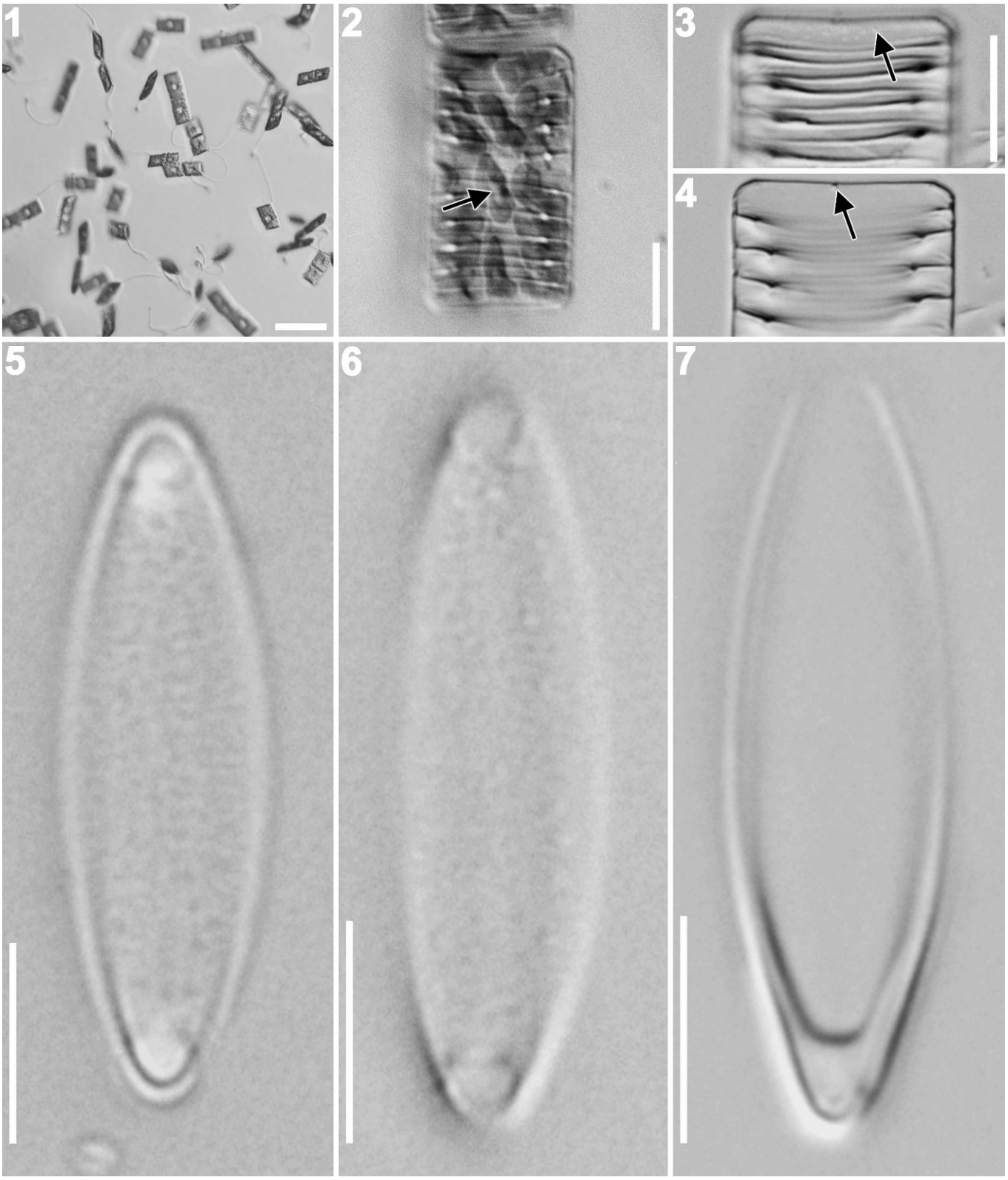

Figs 1–7. *Pseudostriatella oceanica*: living and cleaned cells (LM). Scale bars = 100 μm (Fig. 1), 10 μm (Figs 2, 3) or 5 μm (Figs 5–7).
Fig. 1. Living cells growing in culture vessel.
Fig. 2. Living cell showing multiple plastids. Arrow indicates presumable pyrenoid.
Fig. 3. Cleaned frustule, focused on surface to show prominent ribs along the girdle bands, continuous with the septa. The arrow indicates a white spot on the valve that is probably a rimoportula.
Fig. 4. Median focus of the frustule in Fig. 3, showing septate girdle bands; arrow indicates probable rimoportula.
Fig. 5. Cleaned valve (bright field).
Fig. 6. Cleaned valve (DIC).
Fig. 7. Single girdle band with septum at closed end.

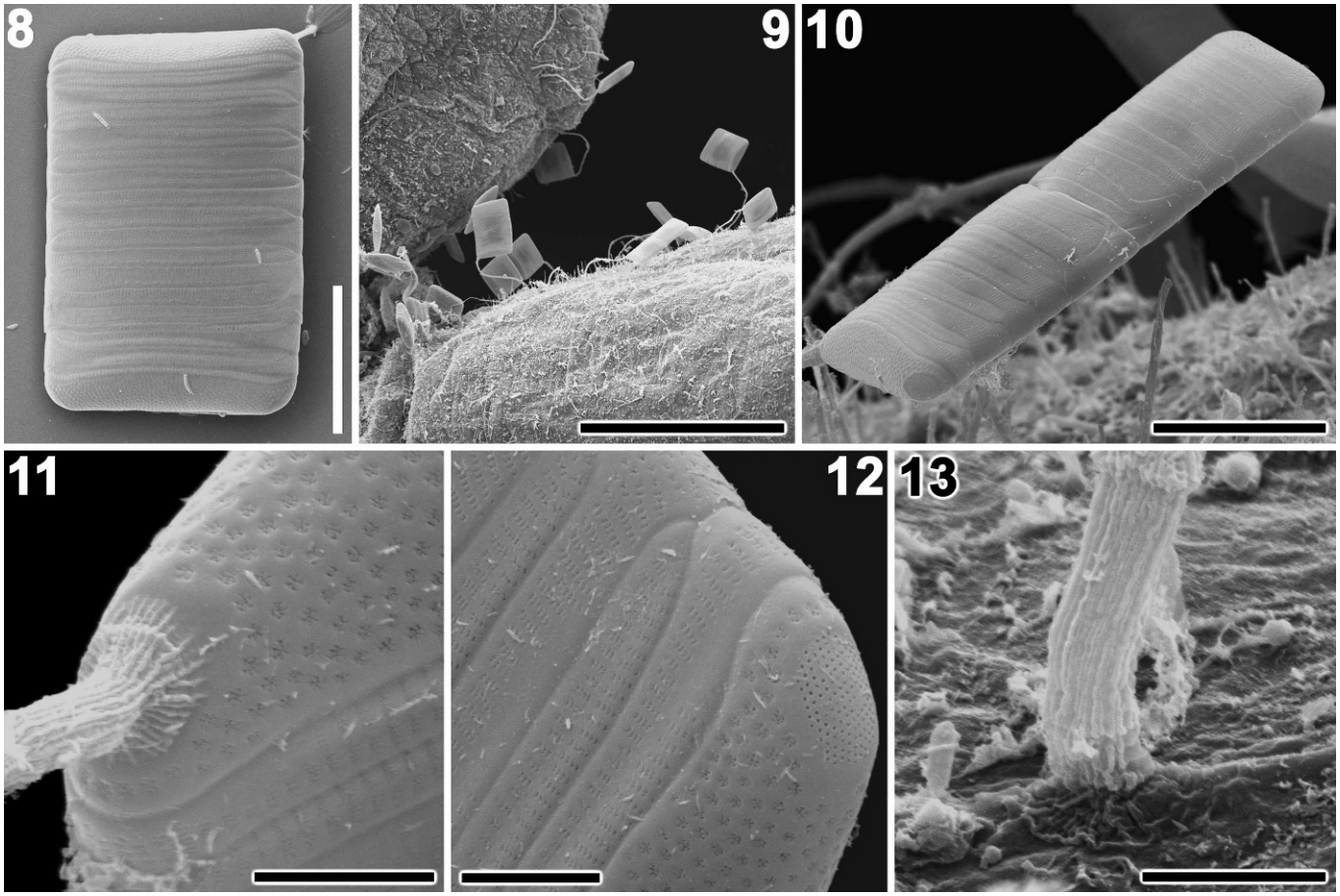

Figs 8–13. *Pseudostriatella oceanica*; intact cells, SEM. Scale bars = 10 μm (Figs 8, 10), 100 μm (Fig. 9) or 2 μm (Figs 11–13).
Fig. 8. Frustule with mucilage stalk secreted at upper right corner.
Fig. 9. Colonies on *Cladophora* sp. Note the cells raised above bacterial community on algal surface by long mucilage stalks.
Fig. 10. Side view of frustules just after cell division.
Fig. 11. Mucilage stalk secreted from apical pore field.
Fig. 12. Free end of valve showing apical pore field secreting no mucilage.
Fig. 13. Mucilage stalk attachment to substratum. Note stalk is composed of fine mucilaginous strings.

at both ends of the valve. They had slightly thickened rims and contained small round pores in a strict hexagonal array (Fig. 16). This structure conforms to the definition of an ocellus (Ross *et al.* 1979). The areolae were more or less isodiametric, and each was occluded by two to several pegs leaving a dendritic aperture (Figs 17, 18).

On the inner surface of the valve, the hyaline area was less obvious than on the exterior but still recognizable (Fig. 19). The peg-like occlusions of the areolae were slightly sunk below the surface internally (Fig. 22), suggesting that these structures were external developments (contrast Figs 17, 18). A few of the pores within the widened ends of the hyaline area penetrated the valve (Fig. 20). The ocelli were not rimmed internally (Fig. 21), in contrast to the external appearance (Fig. 16). Approximately 15–30 rimoportulae were found scattered around the edge of each valve (Figs 19, 23, 24), all of them having a similar size but varying in shape (Figs 25–28). The most common form was 'C-shaped', the lips of the process being continuous on one side. This type of process could be either circular (Fig. 25) or elliptical (Fig. 26). Processes with two entire labiate slits (Fig. 27) were also commonly seen. This bilabiate process is not the same as the bilabiate process in the Lithodesmiales. Rarely, fused processes were observed (Fig. 28). The basal part of each rimoportula always overlapped part of an areola (Figs 25–28). Externally, the openings of the rimoportulae were undetectable (Figs 14–18).

The closed end of each girdle band bore a septum (Fig. 29), which was irregularly perforated by many scattered pores of variable size (Figs 29–31). The pars exterior was perforated by simple slit-like areolae arranged in short striae (Fig. 32); its margins were plain (Fig. 32, arrow and arrowhead, respectively). The closed end of the band was widened in the pervalvar direction to form a ligula (pointing towards the valve) and a smaller antiligula (pointing away from the valve), which were also perforated (Fig. 33). Towards the open ends of the band, the septum became shallower, finally becoming a simple interstria (Fig. 33). The girdle band areolae were slightly sunken internally (Figs 33, 34).

Auxospore structure

Auxosporulation occurred spontaneously in the clonal culture. Nuclear behaviour was not observed in this study,

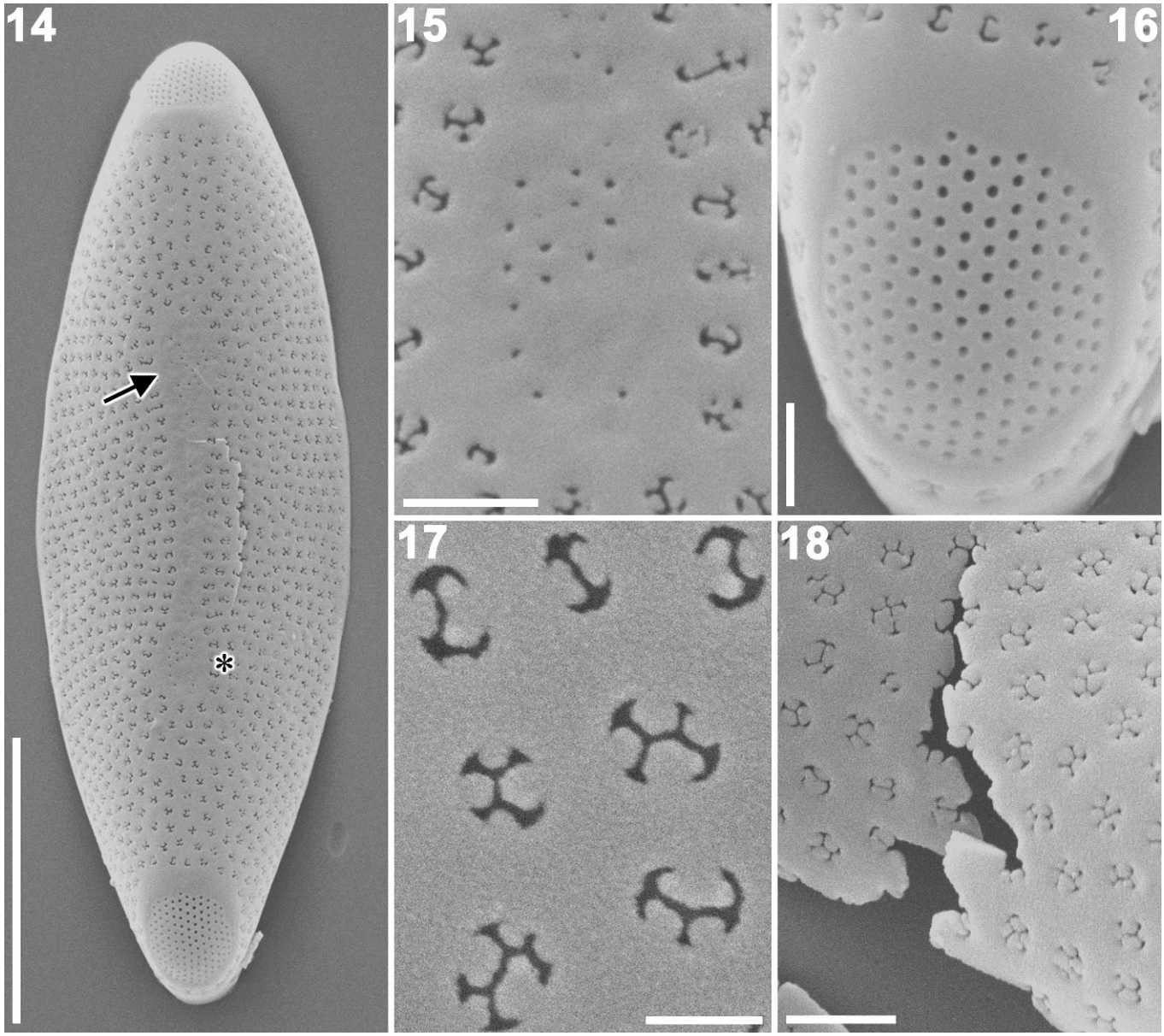

Figs 14–18. *Pseudostriatella oceanica* valves: external views (SEM). Scale bars = 5 μm (Fig. 14), 0.5 μm (Figs 15, 16, 18) or 0.2 μm (Fig. 17).
Fig. 14. Whole showing central hyaline area (arrow) and irregular striation.
Fig. 15. Enlarged view of part marked by asterisk in Fig. 14 showing small simple pores within the end of the hyaline area.
Fig. 16. Detail of apical pore field surrounded by plain rim.
Fig. 17. Areolae occluded by pegs that vary in shape and number.
Fig. 18. Broken valve showing simple nonchambered valve structure.

and the earliest stages directly observed were the dehiscence of the auxospore mother cell, the liberation of the protoplast from its frustule and its bodily movement to a position beyond the open end of one vacated theca (Figs 35–37). The auxospore maintained this position subsequently (Figs 37, 38) and must have been physically connected to the empty mother-cell wall, presumably by mucilage, but the exact nature of the connection could not be established. The young auxospore was more or less spherical (Fig. 37). It then expanded at right angles to the pervalvar axis of the gametangium and parallel to its longitudinal axis (Fig. 38). No perizonial caps were observed at any stage of auxosporulation. All mother cells observed in this study were associated with only a single auxospore (Figs 35–38).

In the earliest stage observed by SEM (Fig. 39), the organic spherical auxospore did not seem to be covered with a mucilage layer or with any siliceous structures. Slightly expanded auxospores (Fig. 40), however, were bordered by a plain fringe of material, which probably represented a delicate mucilaginous envelope (Fig. 41). In auxospores that had already expanded significantly (Figs 42, 43), a striated siliceous structure (Fig. 43) could be seen within the mucilaginous layer (Fig. 43), and this can probably be

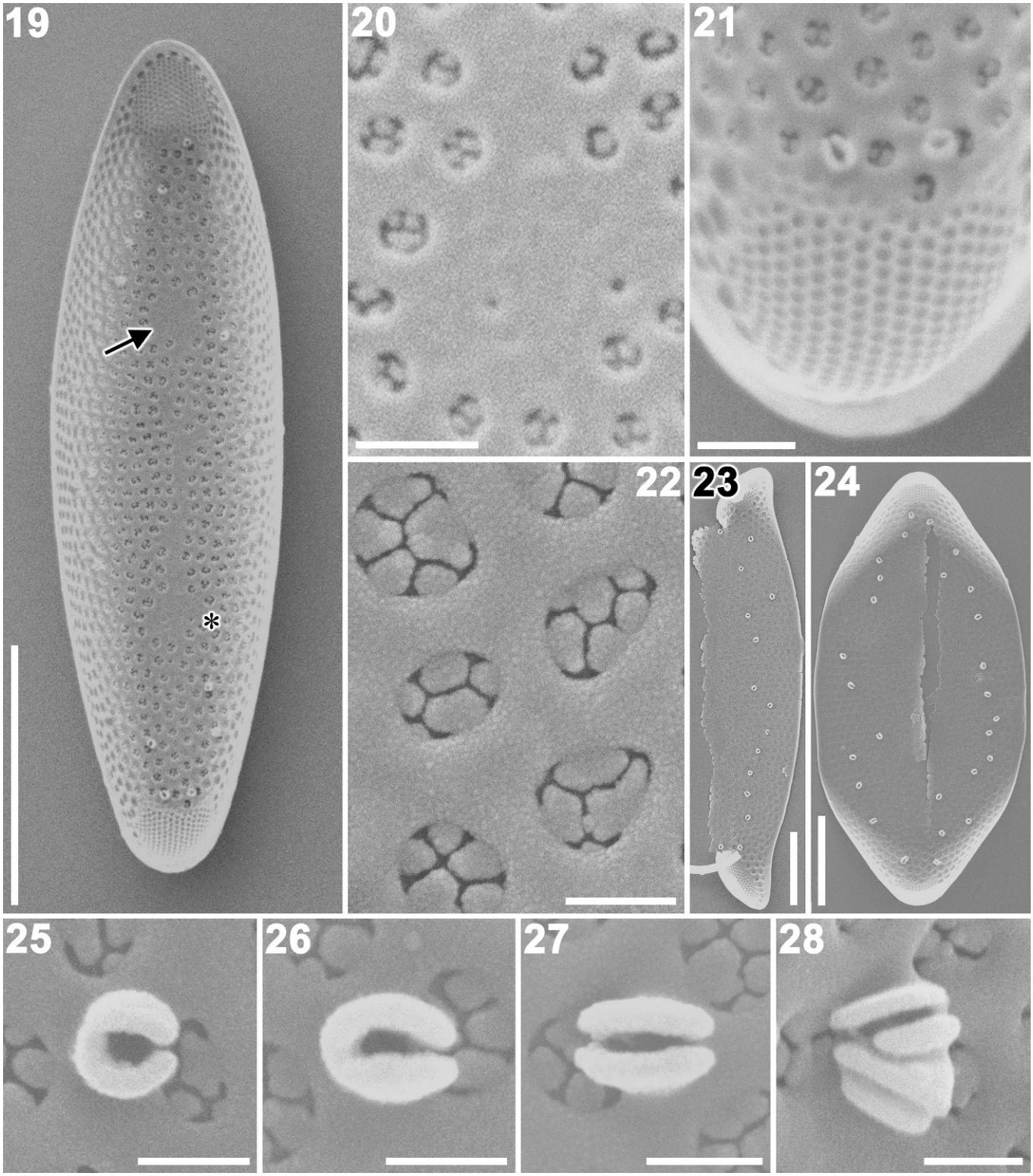

Figs 19–28. *Pseudostriatella oceanica* valves: internal views (SEM). Scale bars = 5 μm (Fig. 19), 0.5 μm (Figs 20, 21), 0.2 μm (Figs 22, 25–28) or 0.3 μm (Figs 23, 24).

Fig. 19. Whole interior. The arrow indicates the hyaline area. Note the many irregularly scattered rimoportulae.
Fig. 20. Enlarged view of part marked by asterisk in Fig. 19 showing a few small, simple pores within the hyaline area.
Fig. 21. Detail of apical pore field.
Fig. 22. Areolae occluded by pegs, which are slightly recessed below the internal valve surface.
Figs 23, 24. Broken valve showing irregularly distributed rimoportulae around the valve margin.
Figs 25, 26. Circular and elliptical C-shaped rimoportulae.
Fig. 27. Normal 'labiate' rimoportula.
Fig. 28. Compound rimoportula.

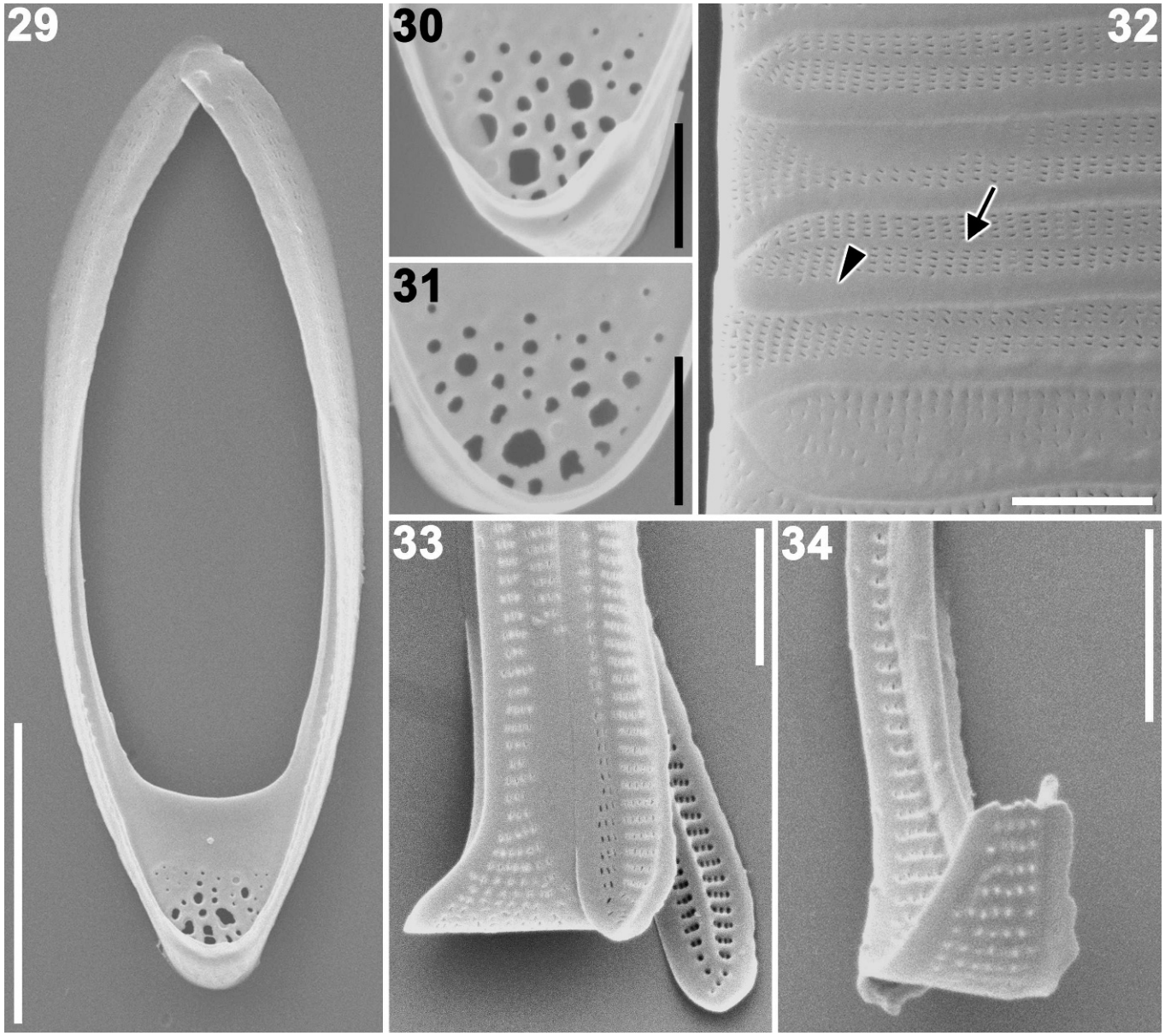

Figs 29–34. *Pseudostriatella oceanica* girdle (SEM). Scale bars = 5 μm (Fig. 29), 1 μm (Figs 30, 31) or 2 μm (Figs 32–34).
Fig. 29. Single band with a perforated septum.
Figs 30, 31. Variation of perforation pattern in septa.
Fig. 32. Complete girdle showing interlocking bands. Note the regular striation, except for a hyaline area along the long axis (arrow) and advalvar edge (arrowhead).
Fig. 33. Disrupted cingulum showing the outside and inside of an open end. (right) and the outside of a closed end. The plain longitudinal strip is thickened and rib-like. Note that the interstriae region are also rib-like.
Fig. 34. Broken copula showing the inside of a closed end. Note that the longitudinal rib becomes more prominent and widens into the septum.

regarded as a longitudinal perizonial (LP) band (*cf.* Fig. 54). No transverse perizonial (TP) bands were seen in this stage. The LP band comprised a longitudinal rib and a series of closely spaced ribs extending out from it at right angles (Fig. 43). At this stage, the body of cell appeared lumpy, which may represent chloroplasts within the auxospore or a partial covering of silica scales (see below).

When the expansion was complete, an initial valve was produced within the auxospore (Fig. 44). By then, the auxospore could be seen to possess not only longitudinal but also transverse bands (Figs 45, 46). The TP bands were very weakly silicified (Figs 45–47) but could be seen to be finely and irregularly porous (Figs 46, 47, 49). Like the first LP band seen earlier in expansion, the TP bands also often consisted of a longitudinal rib bearing transverse ribs (Fig. 47, arrow and arrowhead, respectively), though these were very feebly developed. The ends of the transverse elements of the TP bands sometimes bore a fringe (Fig. 47).

The series of TP bands and LP bands covered the auxospore (Figs 48, 54). We will refer to the side closest to the theca of the auxospore mother cell as 'ventral', and it was on this side that the LP bands lay. There were several

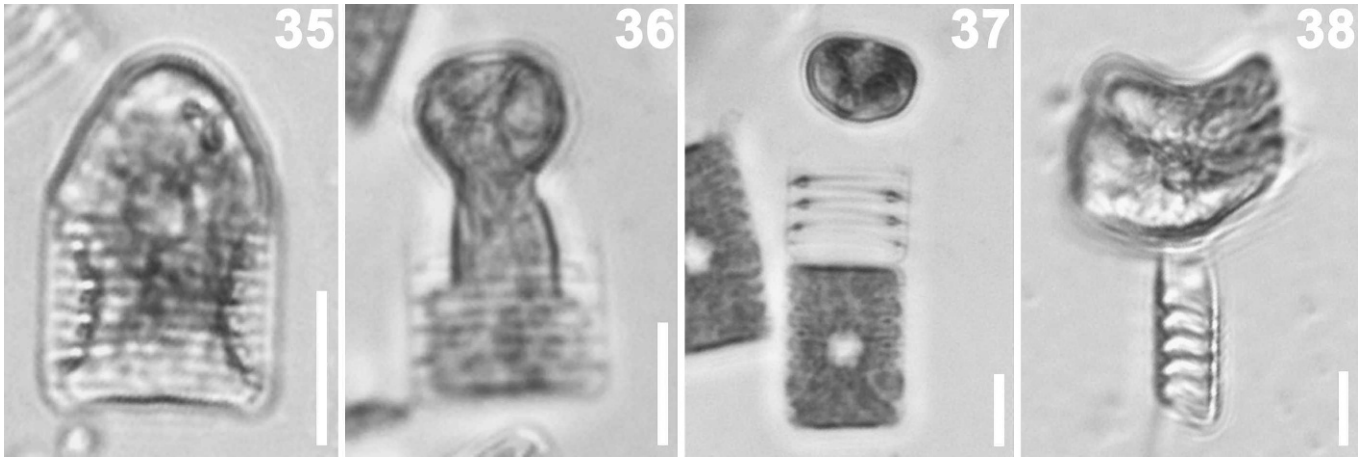

Figs 35–38. *Pseudostriatella oceanica*: clonal auxosporulation (LM). Scale bars = 10 μm.
Figs 35, 36. Young auxospores being liberated from their mother cells.
Fig. 37. Contracted ± spherical auxospore.
Fig. 38. Mature auxospore containing initial cell, lying slightly oblique to the object plane.

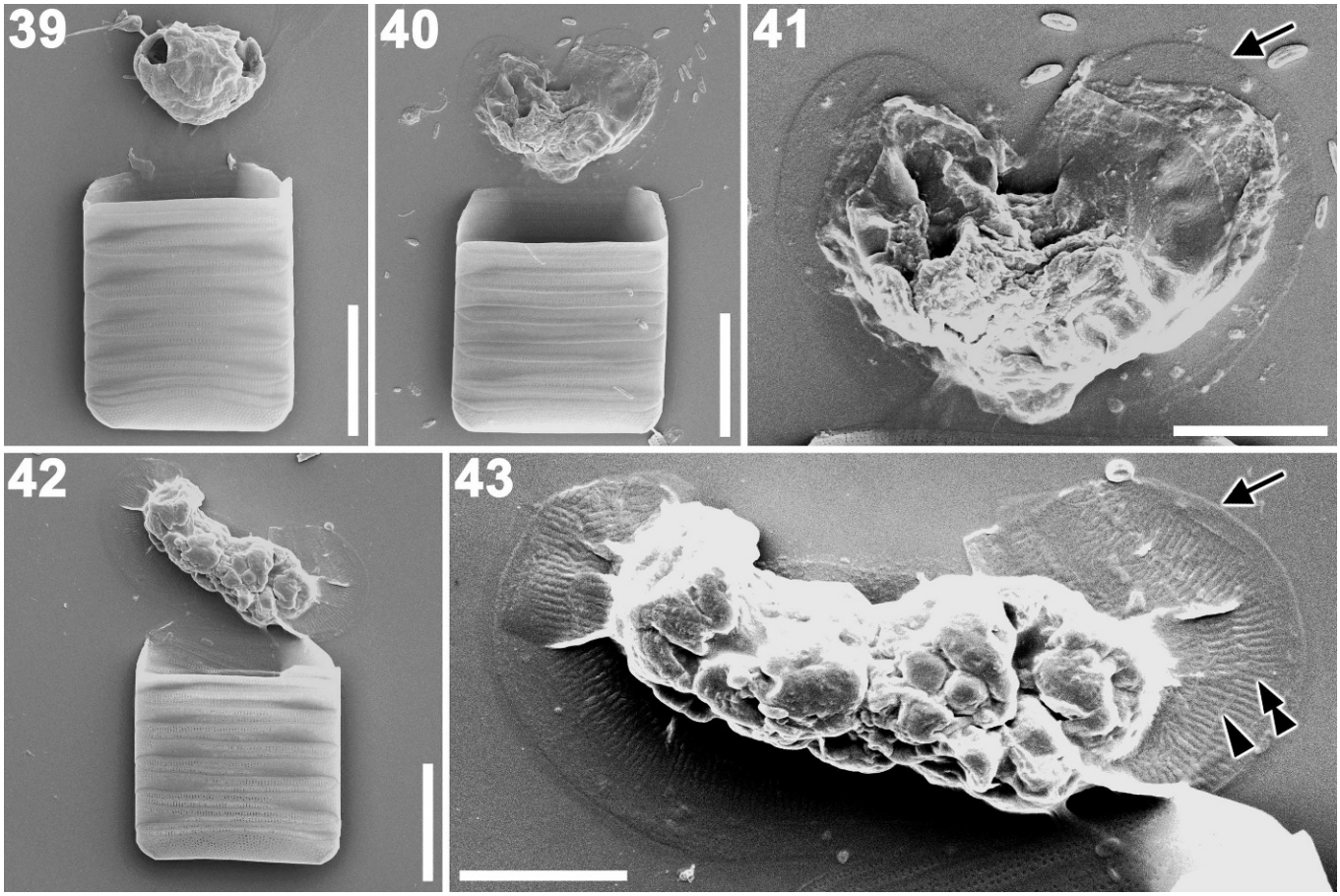

Figs 39–43. *Pseudostriatella oceanica*: early stages of auxosporulation (SEM). Scale bars = 10 μm (Figs 39, 40, 42) or 5 μm (Figs 41, 43).
Fig. 39. Spherical auxospore. No covering is visible.
Fig. 40. Slightly expanded auxospore.
Fig. 41. Enlarged view of auxospore of Fig. 40. Arrow indicates mucilaginous layer covering auxospore.
Fig. 42. Expanding auxospore.
Fig. 43. Enlarged view of auxospore of Fig. 42. Arrow indicates mucilaginous layer. Arrowhead and double arrowhead indicate longitudinal and transverse ribs of a LP band, which has probably been bent during specimen preparation (*cf.* Fig. 54). Note that a transverse perizonium is absent.

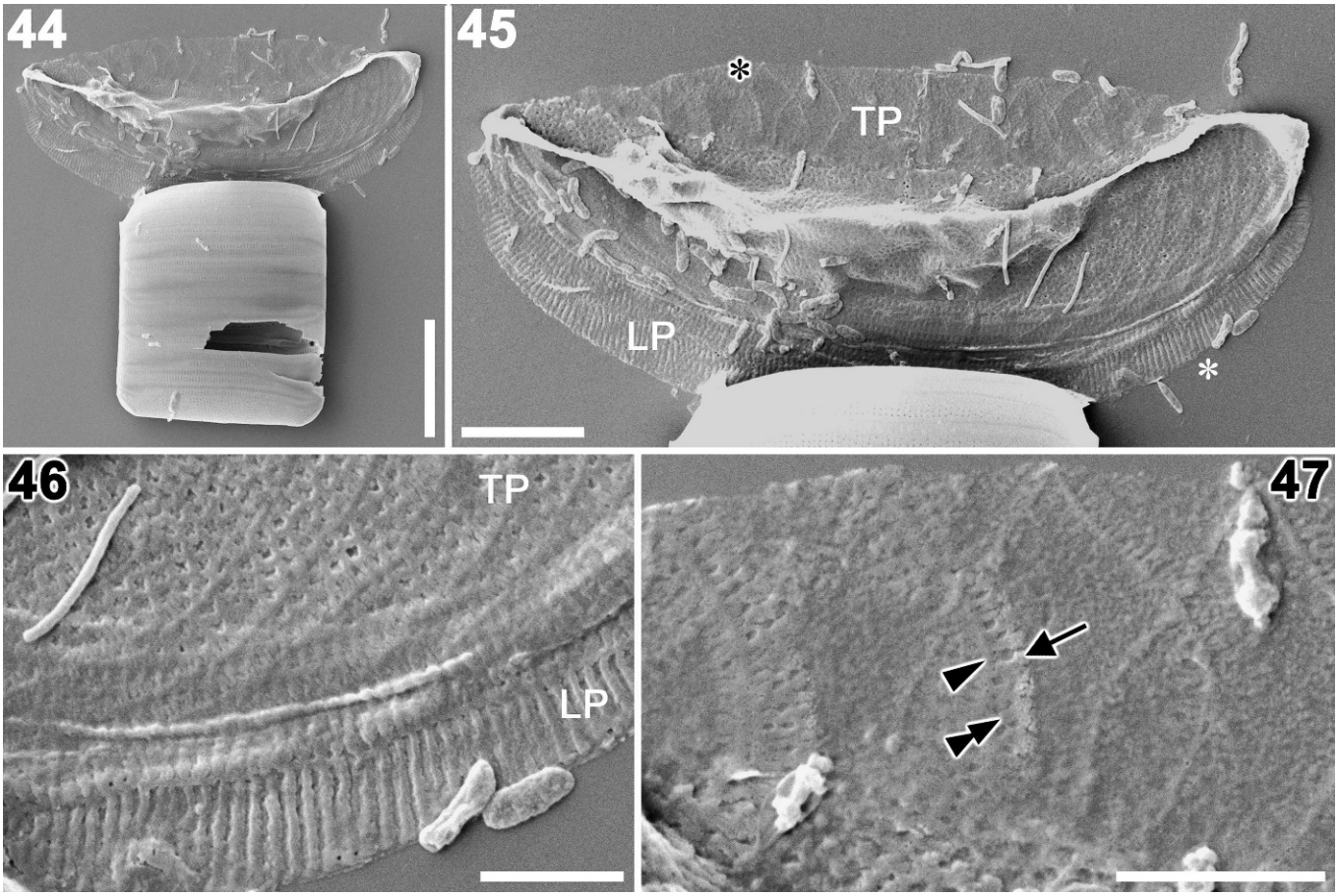

Figs 44–47. *Pseudostriatella oceanica*: fully expanded auxospore containing an immature initial epivalve (SEM). Scale bars = 10 μm (Fig. 44), 5 μm (Fig. 45) or 2 μm (Figs 46, 47).

Fig. 44. Whole auxospore still associated with auxospore mother cell.

Fig. 45. Enlarged view of auxospore: the initial valve is detectable via its larger, coarser areolae, visible along the midline of the collapsed cell. The auxospore is covered by transverse perizonial bands (TP) dorsally and longitudinal perizonial bands (LP) ventrally.

Fig. 46. Enlargement (at black asterisk in Fig. 45), showing the structural differences between the transverse (TP) and longitudinal perizonial bands (LP).

Fig. 47. Enlargement (at white asterisk in Fig. 45), showing the delicate TP bands. No regular striae exist. The arrowhead and double arrowhead indicate the longitudinal and transverse ribs of a TP band, respectively; the arrow indicates a fringe.

TP bands (Fig. 49), all closed hoops except for the primary band, which was a simple strap passing from one side of the auxospore to the other (Fig. 54). The closed hoops, which we will refer to as secondary bands, did not girdle the auxospore fully. Instead, each was divided into two broader segments on the dorsal side of the auxospore, connected by a narrower strip along the ventral side (Figs 49, 54).

The primary band and the adjacent secondary TP band (Fig. 49: '1st' and '2nd', respectively) were so delicate and closely associated that the boundary between them was indistinct, and they may even have been fused together. The more distal TP bands ('3rd' and '4th' in Figs 49, 54) appeared to be slightly more robust than the first two bands and bore distinct longitudinal ribs. The fringed margins of the bands never interlocked with each other (except perhaps between the primary band and its neighbour) but overlapped from the centre outwards, the presumably older bands being external to the younger ones (Fig. 49). Rimoportulae were detected on the initial epivalve (Fig. 49). In fully expanded auxospores, scales were found on the ventral side (Fig. 50). They were thin and delicate and difficult to detect under SEM, unless a strongly contrasted image was produced. They varied in shape, but in the most frequent type there was a central pore field ringed by a prominent annulus bearing a delicate fringe of fine radiating fimbriae (Fig. 50, arrow). Much simpler scales were also found (Fig. 50, arrowhead), lacking the prominent annulus and fringe; they were sometimes fused to each other.

When initial cell formation was complete, the series of TP bands was released from the initial cell (Fig. 51, arrow). There were at least three LP bands. The widest lay furthest towards the ventral side (Fig. 52) and was always flanked in our images by two narrower bands (Figs 52, 53; see also Fig. 54). The transverse ribs of the LP bands were not straight, plain straps but sinuous or branched or even fused (Fig. 53).

Phylogeny

Highly variable regions were excluded from the 18S rDNA alignment. The analysis used 1713 aligned positions, and

for this, *P. oceanica* differed from its closest relative, *S. unipunctata*, in 104 substitutions and 28 indels.

A Bayesian tree inferred from 18S rDNA sequences of 174 diatoms and seven Bolidophyceae (Table 1) confirmed paraphyly for the araphid diatoms within a robust clade of pennate diatoms (Fig. 55). The same result was also obtained with NJ, MP and ML analyses (topologies not shown). Within the pennates, the *Asterionellopsis* Round–*Asteroplanus* Gardner & Crawford–*Talaroneis* Kooistra & De Stefano clade and *Rhaphoneis* cf. *belgica* emerged first, and then a clade containing all other sequenced araphid pennates and a clade of raphid diatoms diverged (Fig. 55; the outgroup centric diatoms and bolidomonads have been omitted for clarity). *Pseudostriatella oceanica* formed a robust monophyly with *S. unipunctata*, this in turn emerging from within raphid diatoms, being sister to the genus *Achnanthes* Bory (MP) or *Eunotia* Ehrenberg (NJ, ML and BI; only the Bayesian tree is shown in Fig. 55).

DISCUSSION

Taxonomic comment on the order Striatellales and the family Striatellaceae

Round *et al.* (1990) proposed that the genus *Striatella* Agardh should be regarded as a monospecific genus because the other (rarely reported) species assigned to it (Van Landingham 1978) differ from the type species *S. unipunctata*. We have encountered and isolated only *S. unipunctata* during this study, and the plastids and fine structure of the other species are unknown. Two of the 12 species considered to be valid by Van Landingham (1978) have been transferred to *Hyalosira* Kützing by Navarro & Williams (1991). There are thus 10 species currently in the genus *Striatella*.

Striatella is the nominate genus of the order Striatellales, which was established by Round *et al.* (1990) and contains the single family Striatellaceae (Kützing 1844). In turn, Round considered the Striatellaceae as comprising three marine benthic genera: *Striatella*, *Hyalosira* and *Grammatophora* Ehrenberg. Judging by the description given by Round *et al.* (1990, p. 655) for the Striatellales, these three genera were linked because they have a narrow or indistinct sternum, well-differentiated apical pore fields (in which the pores are in a strict hexagonal array) and porous septate girdle bands. They also have a rimoportula at each apex. Molecular phylogenies show, however, that although *Hyalosira* and *Grammatophora* form a clade, this does not contain *Striatella*, nor is it a close relative of *Striatella* (Fig. 55; see also Sims *et al.* 2006, fig. 2). These results suggest that the family Striatellaceae and the order Striatellales should contain only the nominate genus *Striatella* and *Pseudostriatella*; the monophyly of this group is strongly supported by 18S rDNA data, and a wider taxonomic revision is currently in preparation using multiple gene markers. With the benefit of hindsight, it is noticeable that *Striatella* differs from *Hyalosira* and *Grammatophora* in the arrangement of the sternum and rimoportula. The rimoportula is adjacent or lateral to the sternum in *Hyalosira* and *Grammatophora* (Round *et al.* 1990; our unpublished observations), but in *Striatella* they are not associated with each other. Instead, the sternum ends some distance short of the apical pore field, and the rimoportula lies within a small area of apically orientated striae. The rimoportulae lie within the striae in *Pseudostriatella* also but are not restricted to the cell apex.

Comparison of *Pseudostriatella* and *Striatella*

There are many morphological and ecological similarities between *P. oceanica* and *S. unipunctata*, such as the numerous copulae and their areolation and prominent septa, the attachment of cells to substrata in the marine littoral and sublittoral by a long mucilaginous stalk and the production of this stalk via a rimmed apical pore field (ocellus). Because of the morphological similarities of *P. oceanica* and *S. unipunctata*, especially with LM, it is quite possible that the species has been misidentified as *S. unipunctata* in the past. On the other hand, there are also many differences, which we regard as sufficient to differentiate these taxa at the rank of genus. The most striking features are the unusual striation, prominent hyaline area, pegged areolae, multiple marginal rimoportulae and perforated septum. Furthermore, if living specimens are obtainable, it is easy to identify them because the plastids of *S. unipunctata* are unmistakable because of their rod shape and radial arrangement (Fig. 56). With care, cleaned material of the genera can also be separated in LM. Thus, in *S. unipunctata*, each corner of the frustule is sharply truncated (Fig. 56) because of the sunken apical pore fields (see Round *et al.* 1990, p. 432, figs d, e); whereas, rounded corners occur in *P. oceanica* (Figs 2–4). Again, in valve views of *S. unipunctata*, the sternum is prominent and runs almost the whole length of the valve, the striae are regularly arranged (with staggered areolae giving a pattern of transversely orientated diamonds) and can be observed (Fig. 57) and the apical rimoportulae are clearly visible; none of these features exist in *P. oceanica* (Figs 5, 6).

Pseudostriatella oceanica is smaller than *S. unipunctata*. The range observed for *P. oceanica* (16.0–47.8 μm) is probably close to the maximum for the species because we observed both auxospore mother cells *and* initial cells. It is possible that smaller cells may be formed on occasion because cells of other species sometimes continue to divide after the minimum threshold for sexual reproduction has been passed (Geitler 1932). Furthermore, the sizes of the initial cells can sometimes depend on the sizes of the gametangia or auxospore mother cells (Davidovich 2001), and this seems to be true in *S. unipunctata* (Chepurnov *in* Roshchin 1994, table 12). However, *S. unipunctata* can attain lengths of more than double the maximum seen in *P. oceanica*. Because *S. unipunctata* is widespread in tropical, subtropical and temperate climate zones (Witkowski *et al.* 2000), there are many records and measurements of this species (e.g. Van Landingham 1978). The widest range, 35–125 μm, is given by Hustedt (1931). Chepurnov *in* Roshchin (1994) observed sexual auxosporulation of *S. unipunctata* in culture and found that gametangia of 32–42 μm gave rise to initial cells of 107–126 μm; in his illustrations the largest auxospore is 154 μm long (measured on his plate 29). In monoclonal cultures (which cannot auxosporulate because

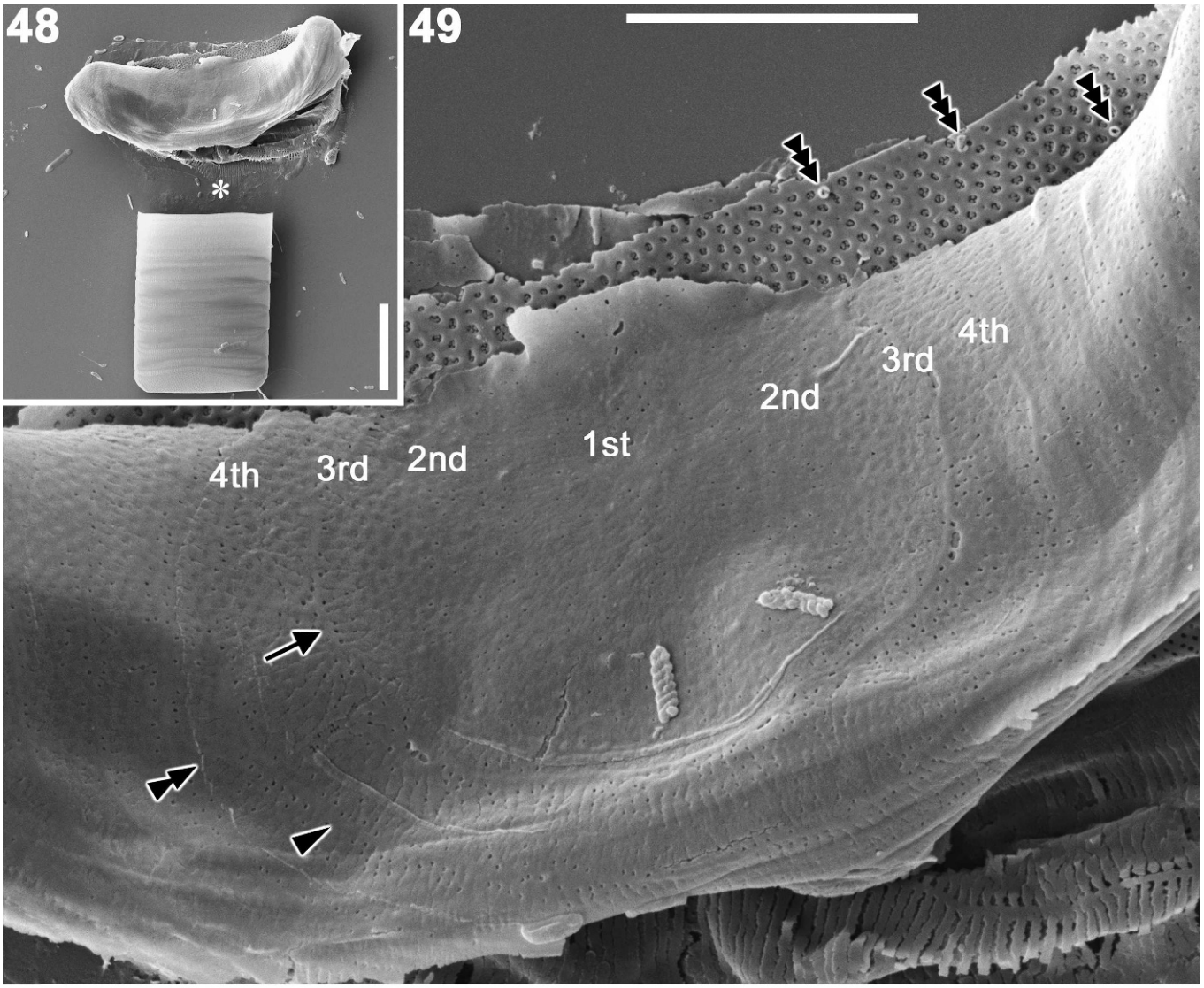
48
49
4th
3rd
2nd
1st
4th
3rd
2nd

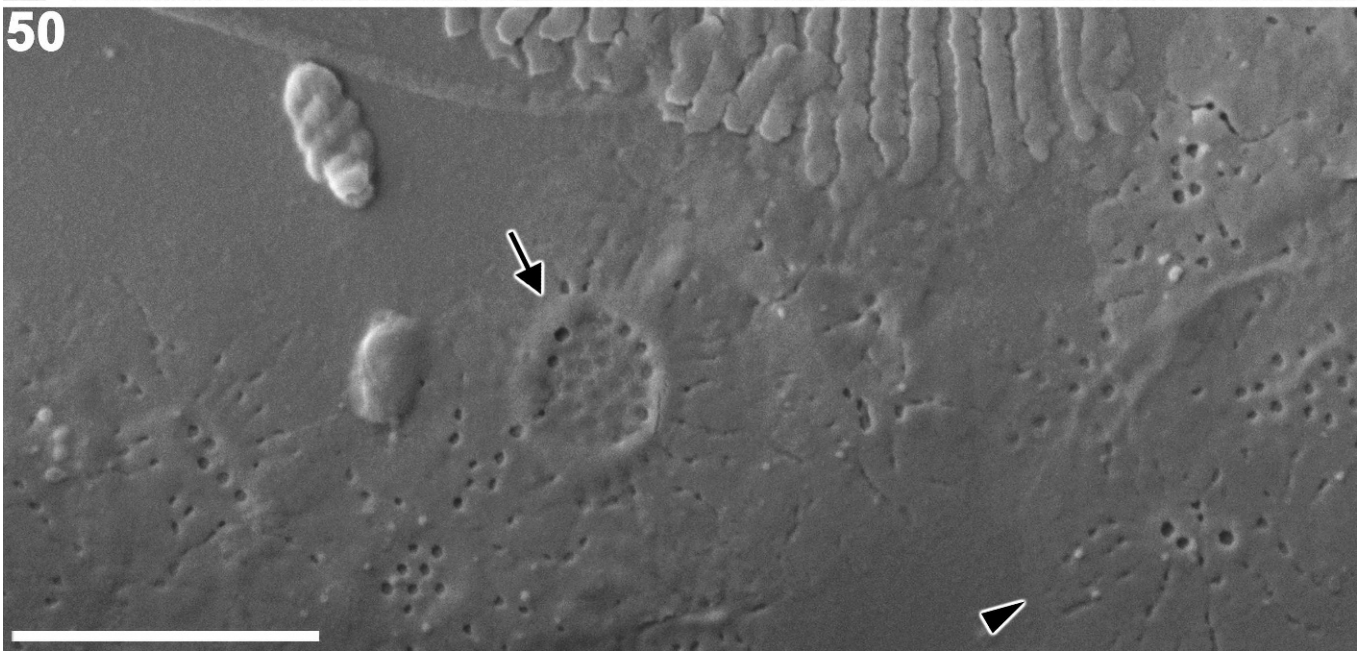
50

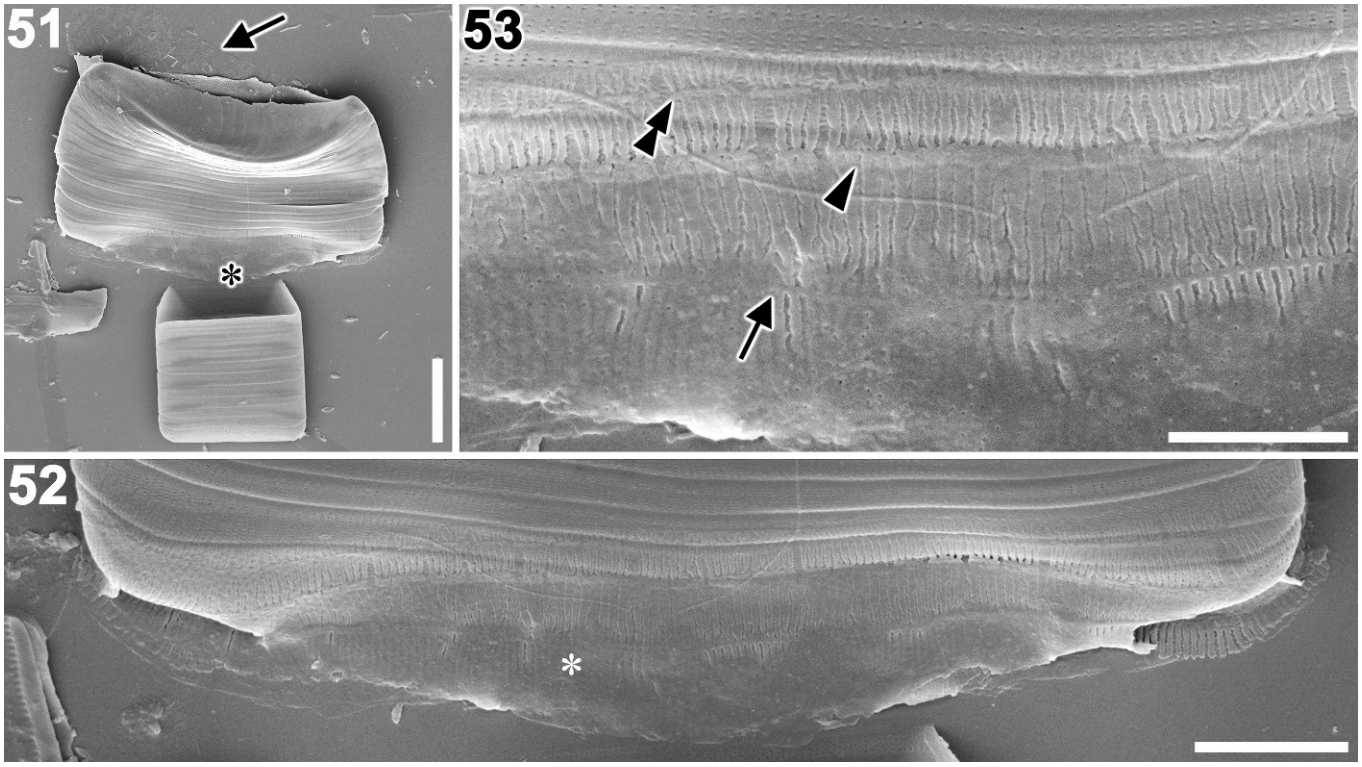

Figs 51–53. *Pseudostriatella oceanica*: initial cell still within auxospore envelope (SEM). Scale bars = 10 μm (Fig. 51), 5 μm (Fig. 52) or 3 μm (Fig. 53).

Fig. 51. Whole initial cell, with auxospore mother cell still attached. The series of TP bands (arrow) appears to be detaching from the initial cell.

Fig. 52. Enlarged view of area marked by black asterisk in Fig. 51, showing the series of LP bands.

Fig. 53. Enlarged view of area marked by white asterisk in Fig. 52. The LP appears to consist of three bands – primary (arrow), secondary (arrowhead) and tertiary (double arrowhead) – but collapse of the auxospore may have hidden two other bands (*cf.* Fig. 54).

S. unipunctata is dioecious), some cells continued to divide until they were 22 μm long before dying. Overall, therefore, although the size ranges of *P. oceanica* and *S. unipunctata* do overlap, they differ enough that valve length can help to distinguish the species in LM.

Rimoportula function

In araphid diatoms, there is some variation in the distribution of the rimoportulae; although, they are most often located along the long axis, mostly near one or both ends of the sternum. Normally, too, each rimoportula has its own special opening externally, which is separate and different from the external openings of the areolae. The consistency of these features suggests that they are maintained by selection, but their significance is unknown because the function of the rimoportula is unclear. In some cases, it has been shown that diatoms secrete mucilage through the rimoportula for movement, as in *Actinocyclus* Ehrenberg (Medlin *et al.* 1986) and *Odontella* Agardh (Pickett-Heaps *et al.* 1986), or adhesion, as in *Melosira* Agardh (Crawford 1975) and *Aulacodiscus* Ehrenberg (Sims & Holmes 1983, p. 270). Schmid (1994) has suggested that the internal part of the rimoportula is used as a cytological anchor for the nucleus during interphase and new valve formation, and recently Kühn & Brownlee (2005) have provided evidence that the rimoportula is a site for endocytosis and therefore involved in membrane recycling. It is quite possible that rimoportulae serve multiple roles in diatoms (Medlin *et al.* 1986). In *P. oceanica*, the rimopor-

←

Figs 48–50. *Pseudostriatella oceanica*: final stage of auxosporulation (SEM). Scale bars = 10 μm (Fig. 48) and 5 μm (Fig. 49) and 2 μm (Fig. 50).

Fig. 48. Auxospore containing a mature initial epivalve.

Fig. 49. Enlarged view of middle of auxospore of Fig. 48, showing that the initial valve is covered by TP and LP (bottom right) bands. TP bands are numbered from primary (1st) to fourth (4th). Note fuzzy border of 1st and 2nd bands. Bands 1 and 2 do not have rib thickenings, whereas bands 3 and 4 bands do (arrow and double arrowhead, respectively). The edge of band 4 overlap onto band 5 (double arrowhead). Triple arrowheads indicate rimoportulae at internal initial valve.

Fig. 50. Enlargement of area marked by asterisk in Fig. 48, showing scales on the ventral side of the auxospore. Two types are present, with (arrow) and without (arrowhead) an annulus.

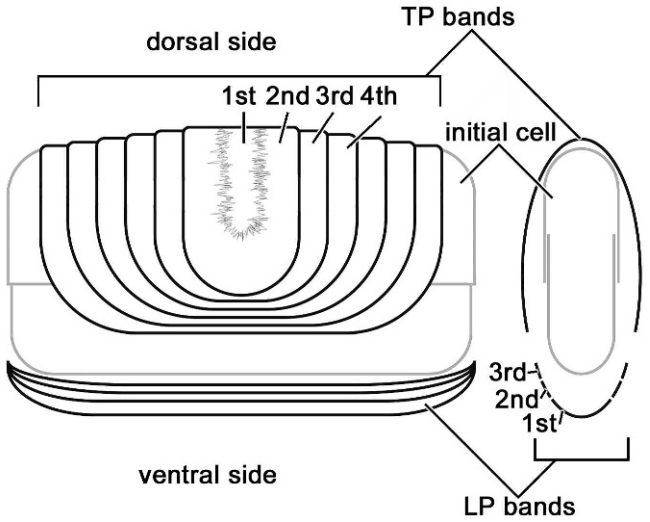

Fig. 54. *Pseudostriatella oceanica*: plan diagram and section (right) of 'perizonium' and initial cell.

tulae have no external openings of their own and connect to the outside instead through part of an areola (Figs 25–28). This, together with their scattered distribution on the valve, makes it unlikely that the rimoportulae function in movement in *P. oceanica* or in the production of robust structured mucilage for adhesion. Altogether, the characteristics of the rimoportulae in *P. oceanica* suggest relaxed functional constraints, relative to other araphid pennates.

On the other hand, the rimoportulae have not been lost altogether in *P. oceanica*, in contrast to members of the Plagiogrammaceae (including *Talaroneis*, *Dimeregramma* Ralfs and *Plagiogramma* Paddock) and other genera, such as *Staurosira* (Ehrenberg) Williams & Round, *Nanofrustulum* Round, Hallsteinsen & Paasche, *Opephora* Petit, *Punctastriata* Williams & Round, *Staurosirella* Mereschkowsky, *Pseudostaurosiropsis* Morales and *Pseudostaurosira* Williams & Round (Round *et al.* 1990, 1999; Morales 2001, 2005; Kooistra *et al.* 2004). Among these rimoportula-lacking diatoms, few seem to be able to grow as epiphytes – possibly only *Talaroneis* (Kooistra *et al.* 2004); the rest grow attached to rocks or sand grains or live planktonically. Possession of rimoportulae may therefore be important in araphid pennates for attachment to plants.

Phylogeny

The 18S rDNA phylogeny gave strong support not only to the monophyly of the *P. oceanica–S. unipunctata* clade (Bootstrap supports in NJ and ML analyses = 100; Bayesian posterior probability = 1.0) but also to the establishment of a new genus for *P. oceanica* because of the long branches connecting both species. The high divergence between these taxa (104 substitutions and 28 indels) contrasts, for example, with the shorter branch lengths within *Grammatophora* Ehrenberg and *Eunotia* (see Fig. 55). We accept, of course, that there is no absolute standard for the amount of sequence difference that justifies generic status. Although *P. oceanica* and *S. unipunctata* lie at the ends of long branches, the possibility that the tree has been distorted by long-branch artifacts can probably be excluded because the two taxa also share a very long node with high statistical support. Preliminary analyses using several gene markers also show that monophyly of the clade containing the two genera is robust (S. Sato, unpublished observations).

Many phylogenetic studies of diatoms made using 18S rDNA have revealed that the araphid pennate diatoms are paraphyletic. They divide into two groups: (1) a relatively small clade of marine diatoms containing the Rhaphoneidaceae, Plagiogrammaceae, *Asterionellopsis* and *Asteroplanus* and (2) a larger, 'core' group (grade) containing the rest of the araphid diatoms that is the sister group to the raphid diatoms (e.g. Medlin & Kaczmarska 2004; Alverson *et al.* 2006; Sims *et al.* 2006). This relationship was recovered in the present analysis. Some features of our tree, such as the sister relationship between the *P. oceanica–S. unipunctata* clade and the raphid genus *Eunotia*, have high support but are frankly implausible because of morphological and reproductive evidence. For example, the pattern of auxosporulation in *Striatella* (*cis* anisogamy coupled with expansion of the auxospore at the mouth of the female gametangium and at right angles to it: Chepurnov *in* Roshchin 1994) is not shared by *Eunotia* (Mann *et al.* 2003) or with any other raphid diatoms (Round *et al.* 1990) but does agree well, though not perfectly, with auxosporulation in *Rhabdonema* Kützing and *Grammatophora* (von Stosch 1962; Sato *et al.* 2008a). There are also no vestiges of a raphe in *Pseudostriatella* (contrast *Cocconeis* Ehrenberg 'pseudoraphe' valves, *Semiorbis* R. Patrick and some *Asterionella*-like diatoms; Mann 1982a; Round *et al.* 1990; Kociolek & Rhode 1998). The poorly supported relationship to the raphid diatoms probably results from well-known analytical artifacts, such as taxon sampling or substitution bias: the long branches seen in *P. oceanica–S. unipunctata* clade suggest an accelerated rate of base substitution, which may make it difficult to reconstruct the phylogeny correctly.

Indeed, 18S rDNA analyses undertaken so far have placed *S. unipunctata* in various phylogenetic positions. Some put the genus at the root of the raphid diatoms (Kooistra *et al.* 2003a, b, 2004). Given the hypothesis of Hasle (1974) that the rimoportula might be the predecessor of the raphe, Kooistra *et al.* (2003a) implied that the slightly elongated external opening of the rimoportula in *Striatella* illustrates how the raphe could have arisen, by elongation towards the centre of the valve, creating two slits splitting the sternum. By contrast, in Medlin & Kaczmarska's (2004) analyses, the sister to *Striatella* is *Staurosira construens* Ehrenberg, which has no morphological features in common with *Striatella* and *Pseudostriatella* beyond its elongate shape (Round *et al.* 1990). In an 18S rDNA tree using almost the same data set of Medlin & Kaczmarska (2004) but constructed by direct optimization (DO), a heuristic maximum parsimony algorithm, *Striatella* is sister to the marine araphid genus *Licmophora* Agardh (Sorhannus 2004). Finally, the genus has appeared within the raphid diatoms, as sister to an *Anomoeoneis* Pfitzer–*Cymbella* Agardh clade (Medlin *et al.* 2000). None of these relationships are robust (i.e. they receive low bootstrap support or Bayesian posterior probabilities; statistical support data are not available in Sorhannus 2004).

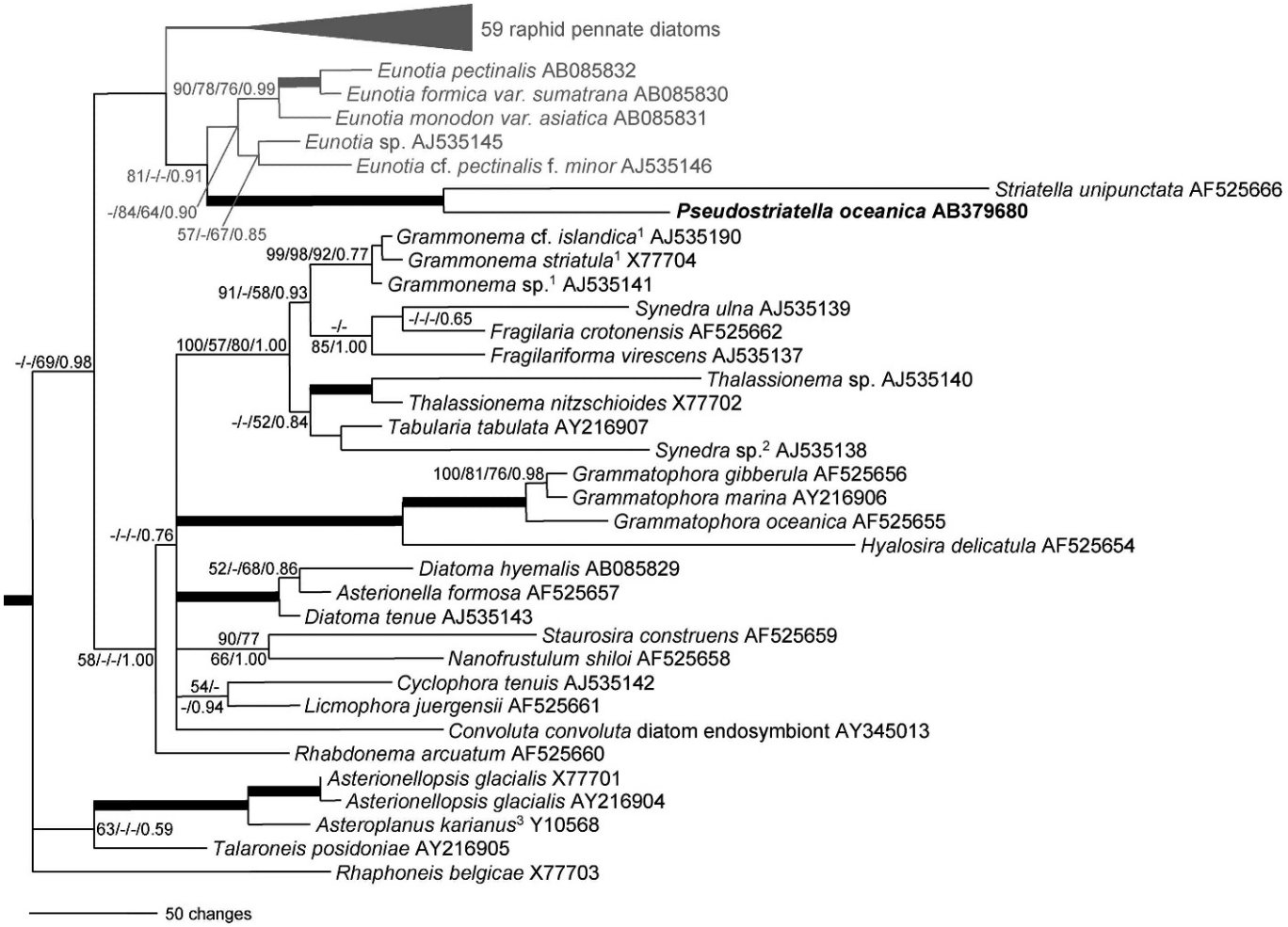

Fig. 55. Molecular phylogeny of araphid pennate diatoms inferred from 18S rDNA sequence using 1713 aligned positions. The tree shown resulted from Bayesian inference using a GTR + I + G model. Outgroup bolidomonads and centric diatoms were excluded, and a clade comprising raphid diatoms is collapsed into triangle for clarity. Nodal support values greater than 50 (NJ, MP and ML) and 0.50 (BI) are shown. Nodes with strong supports (bootstrap support > 90 in NJ, MP and ML, and posterior probability > 0.95 in BI) are shown as thick lines. [1]Name change since deposit; [2]likely a new genus collected from a marine habitat (Medlin et al. 2008a); [3]annotated as *Asterionellopsis kariana* in GenBank.

One recent result from a Bayesian 18S rDNA analysis, using a doublet model that takes base substitutions in rRNA secondary structure into account, constructed a robust *Striatella–Rhabdonema* clade as one of a radiated group of pennate diatoms (Alverson *et al.* 2006, fig. 5). However, the consensus most parsimonious tree disconnected *Striatella* from *Rhabdonema* and put the taxa into polytomy (Alverson *et al.* 2006, fig. 6). Sims *et al.* (2006) used a huge data set that placed *Striatella* at the root of the 'core' araphid + raphid clade with high support. In the ML tree presented by Sorhannus (2007), *Striatella* also diverges at the root of the core araphid clade but with low bootstrap support.

We conclude, therefore, that it is probably impossible at this time to obtain a fully resolved phylogeny resolving the correct phylogenetic placement of the *P. oceanica–S. unipunctata* clade, and it may remain impossible when 18S rDNA sequences are used in a single gene phylogeny. It is particularly important to establish the position of the clade because of the unusual structure of the auxospore (see below) and pattern centre in *P. oceanica*. The pennate diatoms are usually monophyletic in trees based on a variety of genes (molecular studies of diatoms are listed by Mann & Evans 2007), supporting the idea that the 'pennate' Bauplan is a synapomorphy, that is, the possession of a single longitudinal rib-like element (sternum) at the centre of the pattern and deposited first during valve formation, which subtends sets of transverse ribs on either side (e.g. Round *et al.* 1990, p. 31). Some diatoms previously regarded as 'pennates', such as *Toxarium*, *Ardissonea* and *Climacosphenia*, which have a different kind of pattern centre (Mann 1984), have been shown to belong outside the pennate clade (Kooistra *et al.* 2003b; Alverson *et al.* 2006; Medlin *et al.* 2008b). However, the pattern centre in *P. oceanica* is unlike anything found previously in pennate diatoms partly because it is a wide unthickened hyaline area but more importantly because its wider terminal sections contain pores. In fact, the hyaline area resembles a highly elongate annulus – a more extreme version of the elongate annuli seen in some *Odontella* (e.g. Pickett-Heaps *et al.*

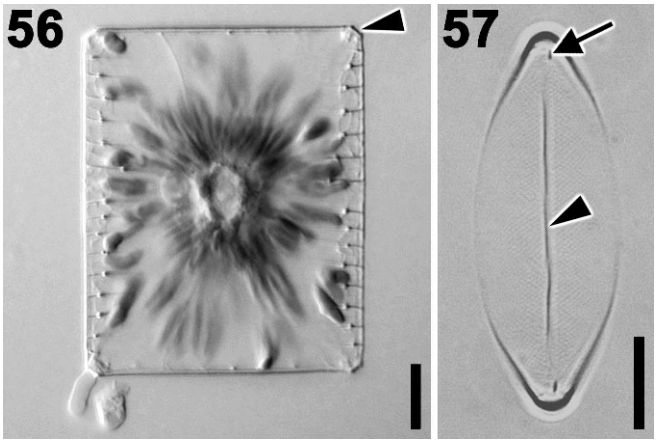

Figs 56, 57. *Striatella unipunctata* (LM). Scale bars = 10 μm.
Fig. 56. Living cell showing distinctive plastids. Arrowhead indicates truncated corner of cell.
Fig. 57. Cleaned valve taken with phase contrast optics. Arrow indicates rimoportula, arrowhead indicates sternum.

1990, fig. 40e) and *Attheya* species (Crawford *et al.* 1994). Until a robust phylogeny is available, it will be unclear whether the resemblance between the *Pseudostriatella* pattern centre and an annulus is a symplesiomorphy (i.e. *Pseudostriatella* does not have and has never had a true sternum) or the result of convergent evolution.

Auxosporulation and auxospore fine structure

We were not able to establish how the auxospores arise in monoclonal cultures of *P. oceanica* because the earliest stages were not seen. It is very unlikely that the auxospores developed through allogamous sexual reproduction because we are confident that we would have observed the empty frustules of any 'male' cells close to the expanding auxospores (Roshchin 1994; Chepurnov *et al.* 2004). Therefore, we have referred to the auxosporulating cells as 'auxospore mother cells' rather than as gametangia. Further work is needed to determine whether auxosporulation involves meiosis and automictic fusion or whether it is apomictic. Nonallogamous formation of auxospores and vegetative cell enlargement has been recorded in other araphid pennates, including *Grammatophora* (Sato *et al.* 2008a) and *Licmophora* (Kumar 1978).

The structure of the auxospore in *P. oceanica* is unlike anything described so far and prompts re-examination of the nature of 'perizonia' and 'properizonia'. In its overall layout, the auxospore casing of *P. oceanica* resembles the envelopes of *Rhabdonema* (von Stosch 1962, 1982), *Gephyria* (Sato *et al.* 2004) and *Grammatophora* (Sato *et al.* 2008a) in that it possesses small more or less isodiametric or slightly elongate scales and also a separate series of longitudinal and transverse bands. However, there are also significant differences, notably in the structure of the transverse bands and the spatiotemporal organization of auxospore development.

There are very few scales in *P. oceanica*, compared to other araphid diatoms (Sato *et al.* 2004, 2008a, b), and we found them only on the mature auxospore (although we cannot wholly exclude that they were present). As in other diatoms (e.g. von Stosch 1962, 1982; Crawford 1974; Kobayashi *et al.* 2001; Schmid & Crawford 2001), the scales varied in shape within a single auxospore. Some scales had an annulus and were morphologically similar to those of centric diatoms (Round *et al.* 1990). In *P. oceanica*, the auxospores never had a complete covering of scales. The few scales present were restricted to the ventral side in nearly mature or mature examples. A ventral distribution is also present in fully developed auxospores of the mediophycean centric diatom *Chaetoceros didymum* Ehrenberg (von Stosch 1982, fig. 2), although here the scales can also be detected from the earliest stages (von Stosch *et al.* 1973; von Stosch 1982).

Some details of perizonial structure were obscured by collapse of the auxospore during air drying. However, the widest LP band was always located at the most ventral end (Fig. 52), and it was associated with two additional bands. We therefore infer that the widest band is the primary band and that the additional bands flanking it are a secondary and a tertiary LP band (Fig. 54). We believe, however, that some of the LP bands were hidden by folding of the auxospore, which seems likely because all of the longitudinal perizonia reported so far in pennate diatoms are structurally symmetrical (e.g. von Stosch 1962, 1982; Mann 1982b; Toyoda *et al.* 2005), even in *Amphora* (Nagumo 2003). There would therefore be five longitudinal bands in *P. oceanica* (Fig. 54), and a similar arrangement has been found in *Tabularia parva* (Sato *et al.* 2008b). Interestingly, even though the valves of *P. oceanica* have a poorly expressed and irregular sternum–stria system, the LP bands have strictly parallel patterning, resembling the striation of normal araphid diatom valves.

The usual structure of the transverse perizonium in pennate diatoms – both araphid and raphid – is that there is a central primary band with a separate series of secondary bands on each side (von Stosch 1982; Mann 1982b). The primary band is either a short cylinder wholly encircling the centre of the auxospore (i.e. it is 'closed': e.g. Poulíčková & Mann 2006), or it is a split ring (an 'open' band) with its ends almost touching (e.g. Sato *et al.* 2004). The secondary bands are usually open, again with their ends closely associated. The TP bands combine to form a cigar-shaped perizonium with a narrow ventral suture, beneath which there is often a set of LP bands, again differentiated into a central primary band and two short flanking series of secondary bands (e.g. Mann 1982b; Mann & Stickle 1993; Nagumo 2003; Sato *et al.* 2004; Toyoda *et al.* 2005). The function of the perizonium appears to be to support and constrain anisometric expansion of the auxospore (Mann 1994).

Many centric diatoms also exhibit anisometric expansion, and again this is apparently controlled through the formation of band-shaped stiffening elements, which together constitute a structure called the 'properizonium' (von Stosch 1982). The key difference between properizonia and perizonia identified by von Stosch (von Stosch & Kowallik 1969; von Stosch *et al.* 1973; von Stosch 1982) is that perizonia are independent from the original zygote wall both structurally and developmentally (the perizonium is 'eine von der ursprünglichen Zygotenhülle unabhängige Struktur': von Stosch & Kowallik 1969, p. 469). In

contrast, properizonia are supposed to be structurally and developmentally continuous with the scale-containing layers that precede them (the otherwise helpful review by Kaczmarska *et al.* 2001 may be misleading in this respect). Thus, von Stosch (1982, p. 146) considered that, for the evolutionary transition from properizonial casings to perizonial diatoms like *Rhabdonema*, 'the first item necessary would be a developmental and spatial hiatus between scale layers and properizonial band systems'. No other features have been identified that are diagnostic for the perizonium vs the properizonium, but it is generally considered (von Stosch 1982; Round *et al.* 1990; Kaczmarska *et al.* 2001; Medlin & Kaczmarska 2004) that perizonia are characteristic of pennate diatoms; whereas, properizonia are restricted to some lineages of multipolar centric diatoms. Our observations of *P. oceanica* revealed no clear developmental separation between a primary scale-bearing wall and the 'perizonium'. Scales were rare and produced apparently only towards the end of auxospore expansion, and it appears too that longitudinal perizonial elements are produced before the transverse perizonium. In retrospect, we believe that a similar continuity of development may occur also in *Gephyria*, where we (Sato *et al.* 2004) detected scales on the inside of the primary TP band.

Another curious, 'transitional' feature of *P. oceanica* auxospores concerns the nature of the secondary TP bands. As noted above, the secondary bands on either side of the primary TP band are separate entities in the perizonia of all raphid and araphid pennates studied until now, as they are also in a few properizonia (those of *Odontella* and *Biddulphia*; von Stosch 1982). *Pseudostriatella* is quite different because the secondary TP elements are continuous from one end of the auxospore to the other around the ventral side (Fig. 54). Each is therefore a complex hoop, shaped like the margin of a saddle. Thus, although the expansion of the auxospore is bipolar in *P. oceanica*, the development of the TP itself is unipolar, beginning from the strap-like primary band and extending out both laterally (towards the poles) and ventrally. Exactly the same unipolar pattern of development occurs in the properizonia of *Chaetoceros*, *Bacteriastrum*, *Attheya*, *Lithodesmium* (here the topology is more complex, because most auxospores are triradiate) and *Bellerochea* (von Stosch 1982) and also in *Lampriscus* (Idei & Nagumo 2002). Thus, it would be as reasonable to regard the auxospore casing of *P. oceanica* as a properizonium as it is to describe it as a true perizonium, despite the fact that this species clearly belongs phylogenetically to the pennate lineage. The presence of longitudinal elements in the *Pseudostriatella* casing is not conclusive support for interpretation as a perizonium because (1) longitudinal elements are present beneath the 'transverse' bands in the triradiate centric *Lithodesmium* (von Stosch 1982; see also Round *et al.* 1990) and (2) the longitudinal bands of *P. oceanica* seem to be formed before the transverse bands, whereas during perizonium formation in raphid diatoms the converse is true.

A simple conclusion can be drawn: there is simply too little information from too few taxa to allow detailed analysis of the evolution of auxospore structure, and the distinction between properizonia and perizonia needs to be re-evaluated. All that can be said at the moment is that classification into scaly, properizonial and perizonial auxospores (*cf.* the 'isometric', 'anisometric' and 'bilateral' auxospores of Kaczmarska *et al.* 2001) is perhaps too simple but that the development of shape *is* generally associated with stiffening of the auxospore wall during expansion by silica bands and hoops.

ACKNOWLEDGEMENTS

The authors are grateful to Beth K. Petkus for collection of living specimen and brought us it from the United States to Germany with her, Richard M. Crawford for correction of the manuscript and discussion, Stephan Frickenhaus for establishing parallel processing for Bayesian analyses, Paul A. Fryxell for helping to translate the Latin diagnosis, Friedel Hinz for technical help for LM and SEM, and Masahiko Idei for allowing us to access his poster for the 17th International Diatom Symposium. We also thank two anonymous reviewers for their valuable comments and suggestions. This study was supported by DAAD for doctoral research fellowship to Shinya Sato.

REFERENCES

Altekar G., Dwarkadas S., Huelsenbeck J.P. & Ronquist F. 2004. Parallel Metropolis-coupled Markov chain Monte Carlo for Bayesian phylogenetic inference. *Bioinformatics* 20: 407–415.

Alverson A.J., Cannone J.J., Gutell R.R. & Theriot E.C. 2006. The evolution of elongate shape in diatoms. *Journal of Phycology* 42: 655–668.

Amato A., Orsini L., D'Alelio D. & Montresor M. 2005. Life cycle, size reduction patterns, and ultrastructure of the pennate planktonic diatom *Pseudo-nitzschia delicatissima* (Bacillariophyta). *Journal of Phycology* 41: 542–556.

Anonymous. 1975. Proposals for a standardization of diatom terminology and diagnoses. *Nova Hedwigia, Beiheft* 53: 323–354.

Cahoon L.B. 1999. The role of benthic microalgae in neritic ecosystems. *Oceanography and Marine Biology. An Annual Review* 37: 47–86.

Chepurnov V.A., Mann D.G., Sabbe K. & Vyverman W. 2004. Experimental studies on sexual reproduction in diatoms. *International Review of Cytology* 237: 91–154.

Cohn S.A., Spurck T.P., Pickett-Heaps J.D. & Edgar L.A. 1989. Perizonium and initial valve formation in the diatom *Navicula cuspidata* (Bacillariophyceae). *Journal of Phycology* 25: 15–26.

Crawford R.M. 1974. The auxospore wall of the marine diatom *Melosira nummuloides* (Dillw.) C. Ag. and related species. *British Phycological Journal* 9: 9–20.

Crawford R.M. 1975. The frustule of the initial cells of some species of the diatom genus *Melosira* C. Agardh. *Nova Hedwigia, Beiheft* 53: 37–50.

Crawford R.M., Gardner C. & Medlin L.K. 1994. The genus *Attheya*. I. A description of four new taxa, and the transfer of *Gonioceros septentrionalis* and *G. armatus*. *Diatom Research* 9: 27–51.

Davidovich N.A. 2001. Species-specific sizes and size range of sexual reproduction in diatoms. In: *Proceedings of the 16th International Diatom Symposium* (Ed. by A. Economou-Amilli), University of Athens, Greece. pp. 191–196.

Elwood H.J., Olsen G.J. & Sogin M.L. 1985. The small subunit ribosomal DNA gene sequences from the hypotrichous ciliates *Oxytricha nova* and *Stylonichia pustulata*. *Molecular Biology and Evolution* 2: 399–410.

EPPLEY R.W., HOLMES R.W. & STRICKLAND J.D.H. 1967. Sinking rates of the marine phytoplankton measured with a fluorochrometer. *Journal of Experimental Marine Biology and Ecology* 1: 191–208.

GEITLER L. 1932. Der Formwechsel der pennaten Diatomeen. *Archiv für Protistenkunde* 78: 1–226.

GILLESPIE J.J., MCKENNA C.H., YODER M.J., GUTELL R.R., JOHNSTON J.S., KATHIRITHAMBY J. & COGNATO A.I. 2005. Assessing the odd secondary structural properties of nuclear small subunit ribosomal RNA sequences (SSU) of the twisted-wing parasites (Insecta: Strepsiptera). *Insect Molecular Biology* 14: 625–643.

GUILLOU L., CHRÉTIENNOT-DINET M.-J., MEDLIN L.K., CLAUSTRE H., LOISEAUX-DE GOËR S. & VAULOT D. 1999. *Bolidomonas*: a new genus with two species belonging to a new algal class, the Bolidophyceae class. nov. (Heterokonta). *Journal of Phycology* 35: 368–381.

HALL T.A. 1999. BioEdit: a user-friendly biological sequence alignment editor and analysis program for Windows 95/98/NT. *Nucleic Acids Symposium Series* 41: 95–98.

HANCOCK J.M. & VOGLER A.P. 2000. How slippage-derived sequences are incorporated into rRNA variable-region secondary structure: implications for phylogeny reconstruction. *Molecular Phylogenetics and Evolution* 14: 366–374.

HASLE G.R. 1974. The 'mucilage pore' of pennate diatoms. *Nova Hedwigia, Beiheft* 45: 167–194.

HUELSENBECK J.P. & RONQUIST F. 2001. MRBAYES: Bayesian inference of phylogeny. *Bioinformatics* 17: 754–755.

HUSTEDT F. 1931. Die Kieselalgen Deutschlands, Österreichs und der Schweiz. In: *Dr L Rabenhorsts Kryptogamenflora von Deutschland, Österreich und der Schweizvol*, vol. 7(2:1). Akademische Verlagsgesellschaft, Leipzig, Germany. pp. 1–176.

IDEI M. & NAGUMO T. 2002. Auxospore structure of the marine diatom genus *Lampriscus* with triangular/quadrangular forms. In: *Abstracts, 17th International Diatom Symposium* (Ed. by M. Poulin), Ottawa, Canada. 166 pp.

KACZMARSKA I., BATES S.S., EHRMAN J.M. & LÉGER C. 2000. Fine structure of the gamete, auxospore and initial cell in the pennate diatom *Pseudo-nitzschia multiseries* (Bacillariophyta). *Nova Hedwigia* 71: 337–357.

KACZMARSKA I., EHRMAN J.M. & BATES S.S. 2001. A review of auxospore structure, ontogeny and diatom phylogeny. In: *Proceedings of the 16th International Diatom Symposium* (Ed. by A. Economou-Amilli), University of Athens, Greece. pp. 153–168.

KOBAYASHI A., OSADA K., NAGUMO T. & TANAKA J. 2001. An auxospore of *Arachnoidiscus ornatus* Ehrenberg. In: *Proceedings of the 16th International Diatom Symposium* (Ed. by A. Economou-Amilli), University of Athens, Greece. pp. 197–204.

KOCIOLEK J.P. & RHODE K. 1998. Raphe vestiges in *Asterionella* species from Madagascar: evidence for a polyphyletic origin of the araphid diatoms? *Cryptogamie: Algologie* 19: 57–74.

KOOISTRA W.H.C.F., DE STEFANO M., MANN D.G. & MEDLIN L.K. 2003a. The phylogeny of the diatoms. *Progress in Molecular and Subcellular Biology* 33: 59–97.

KOOISTRA W., DE STEFANO M., MANN D.G., SALMA N. & MEDLIN L.K. 2003b. Phylogenetic position of *Toxarium*, a pennate-like lineage within centric diatoms (Bacillariophyceae). *Journal of Phycology* 39: 185–197.

KOOISTRA W.H.C.F., FORLANI G., STERRENBURG F.A.S. & DE STEFANO M. 2004. Molecular phylogeny and morphology of the marine diatom *Talaroneis posidoniae* gen. et sp. nov. (Bacillariophyta) advocate the return of the Plagiogrammaceae to the pennate diatoms. *Phycologia* 43: 58–67.

KÜHN S.F. & BROWNLEE C. 2005. Membrane organisation and dynamics in the marine diatom *Coscinodiscus wailesii* (Bacillariophyceae). *Botanica Marina* 48: 297–305.

KUMAR R. 1978. Auxospore formation in species of the marine diatom *Licmophora* Agardh. *Veröffentlichungen des Instituts für Meeresforschungen in Bremerhaven* 17: 15–20.

KÜTZING F.T. 1844. *Die kieselschaligen Bacillarien oder Diatomeen*. Nordhausen, Germany. 152 pp.

MANN D.G. 1982a. Structure, life history and systematics of *Rhoicosphenia* (Bacillariophyta) I. The vegetative cell of *Rh. curvata*. *Journal of Phycology* 18: 162–176.

MANN D.G. 1982b. Structure, life history and systematics of *Rhoicosphenia* (Bacillariophyta). II. Auxospore formation and perizonium structure of *Rh. curvata*. *Journal of Phycology* 18: 264–274.

MANN D.G. 1984. An ontogenetic approach to diatom systematics. In: *Proceedings of the 7th International Diatom Symposium* (Ed. by D.G. Mann), O. Koeltz, Koenigstein, Germany. pp. 113–144.

MANN G.D. 1994. The origins of shape and form in diatoms: the interplay between morphogenetic studies and systematics. In: *Shape and form in plants and fungi* (Ed. by D.S. Ingram & A.J. Hudson), Academic Press, London. pp. 17–38.

MANN D.G. & EVANS M.K. 2007. Molecular genetics and the neglected art of diatomics. In: *Unravelling the algae – the past, present and future of algal molecular systematics* (Ed. by J. Brodie & J.M. Lewis), CRC Press, Boca Raton, FL, USA. pp. 232–266.

MANN D.G. & STICKLE A.J. 1993. Life history and systematics of *Lyrella*. *Nova Hedwigia, Beiheft* 106: 43–70.

MANN D.G., CHEPURNOV V.A. & IDEI M. 2003. Mating system, sexual reproduction and auxosporulation in the anomalous raphid diatom *Eunotia* (Bacillariophyta). *Journal of Phycology* 39: 1067–1084.

MEDLIN L.K. & KACZMARSKA I. 2004. Evolution of the diatoms: V. Morphological and cytological support for the major clades and a taxonomic revision. *Phycologia* 43: 245–270.

MEDLIN L.K., CRAWFORD R.M. & ANDERSEN R.A. 1986. Histochemical and ultrastructural evidence for the function of the labiate process in the movement of centric diatoms. *British Phycological Journal* 21: 297–301.

MEDLIN L., ELWOOD H.J., STICKEL S. & SOGIN M.L. 1988. The characterization of enzymatically amplified eukaryotic 16S-like rRNA coding regions. *Gene* 71: 491–499.

MEDLIN L.K., KOOISTRA W.H.C.F. & SCHMID A.M.-M. 2000. A review of the evolution of the diatoms – a total approach using molecules, morphology and geology. In: *The origin and early evolution of the diatoms: fossil, molecular and biogeographical approaches* (Ed. by A. Witkowski & J. Sieminska), Szafer Institute of Botany, Polish Academy of Science, Cracow, Poland. pp. 13–35.

MEDLIN L.K., JUNG I., BAHULIKAR R., MENDGEN K., KROTH P. & KOOISTRA W.H.C.F. 2008a. Evolution of the diatoms. VI. Assessment of the new genera in the araphids using molecular data. *Nova Hedwigia* 133: 81–100.

MEDLIN L.K., SATO S., MANN D.G. & KOOISTRA W.H.C.F. 2008b. Molecular evidence confirms sister relationship of *Ardissonea*, *Climacosphenia* and *Toxarium* within the bipolar centric diatoms (Bacillariophyta, Mediophyceae) and cladistic analyses confirms that extremely elongated shape has arisen twice in the diatoms *Journal of Phycology*: in press.

MORALES E. 2001. Morphological studies in selected fragilarioid diatoms (Bacillariophyceae) from Connecticut waters (U.S.A.). *Proceedings of the Academy of Natural Sciences of Philadelphia* 151: 39–54.

MORALES E. 2005. Observations of the morphology of some known and new fragilarioid diatoms (Bacillariophyceae) from rivers in the USA. *Phycological Research* 53: 113–133.

NAGUMO T. 2003. Taxonomic studies of the subgenus *Amphora* Cleve of the genus *Amphora* (Bacillariophyceae) in Japan. *Bibliotheca Diatomologica* 49: 1–265.

NAGUMO T. & KOBAYASHI H. 1990. The bleaching method for gently loosening and cleaning a single diatom frustule. *Diatom* 5: 45–50.

NAVARRO N.J. & WILLIAMS D.M. 1991. Description of *Hyalosira tropicalis* sp. nov. (Bacillariophyta) with notes on the status of *Hyalosira* Kützing and *Microtabella* Round. *Diatom Research* 6: 327–336.

PICKETT-HEAPS J.D., HILL D.R.A. & WETHERBEE R. 1986. Cellular movement in the centric diatom *Odontella sinensis*. *Journal of Phycology* 22: 334–339.

PICKETT-HEAPS J.D., SCHMID A.-M.M. & EDGAR L.A. 1990. The cell biology of diatom valve formation. *Progress in Phycological Research* 7: 1–168.

POSADA D. & CRANDALL K.A. 1998. Modeltest: testing the model of DNA substitution. *Bioinformatics* 14: 817–818.

POULIČKOVÁ A. & MANN D.G. 2006. Sexual reproduction in *Navicula cryptocephala* (Bacillariophyceae). *Journal of Phycology* 42: 872–886.

POULIČKOVÁ A., MAYAMA S., CHEPURNOV V.A. & MANN D.G. 2007. Heterothallic auxosporulation, incunabula and perizonium in *Pinnularia* (Bacillariophyceae). *European Journal of Phycology* 42: 367–390.

RONQUIST F. & HUELSENBECK J.P. 2003. MrBayes 3: Bayesian phylogenetic inference under mixed models. *Bioinformatics* 19: 1572–1574.

ROSHCHIN A.M. 1994. *Zhiznennye tsikly diatomovykh vodoroslej*. Naukova Dumka, Kiev. 170 pp.

ROSS R., COX E.J., KARAYEVA N.I., MANN D.G., PADDOCK T.B.B., SIMONSEN R. & SIMS P.A. 1979. An amended terminology for the siliceous components of the diatom cell. *Nova Hedwigia, Beiheft* 64: 513–533.

ROUND F.E., CRAWFORD R.M. & MANN D.G. 1990. *The diatoms: biology and morphology of the genera*. Cambridge University Press, Cambridge, UK. 747 pp.

ROUND F.E., HALLSTEINSEN H. & PAASCHE E. 1999. On a previously controversial ''fragilarioid'' diatom now placed in a new genus *Nanofrustulum*. *Diatom Research* 14: 343–356.

SATO S., NAGUMO T. & TANAKA J. 2004. Auxospore formation and the morphology of the initial cell of the marine araphid diatom *Gephyria media* (Bacillariophyceae). *Journal of Phycology* 40: 684–691.

SATO S., MANN D.G., NAGUMO T., TANAKA J. & MEDLIN L.K. 2008a. Life cycle of *Grammatophora marina* (Bacillariophyta) with special reference to its auxospore fine structure. *Phycologia* 47: 12–27.

SATO S., KURIYAMA K., TADANO T. & MEDLIN K.L. 2008b. Auxospore fine structure in a marine araphid diatom *Tabularia parva* (Bacillariophyta). *Diatom Research*. In press.

SCHMID A.-M.M. 1994. Aspects of morphogenesis and function of diatom cell walls with implications for taxonomy. *Protoplasma* 181: 43–60.

SCHMID A.-M.M. & CRAWFORD R.M. 2001. *Ellerbeckia arenaria* (Bacillariophyceae): formation of auxospores and initial cells. *European Journal of Phycology* 36: 307–320.

SHULL V.L., VOGLER A.P., BAKER M.D., MADDISON D.R. & HAMMOND P.M. 2001. Sequence alignment of 18S ribosomal RNA and the basal relationships of adephagan beetles: evidence for monophyly of aquatic families and the placement of Trachypachidae. *Systematic Biology* 50: 945–969.

SIMS P.A. & HOLMES R.W. 1983. Studies on the ''kittonii'' group of *Aulacodiscus* species. *Bacillaria* 6: 267–292.

SIMS P.A., MANN D.G. & MEDLIN L.K. 2006. Evolution of the diatoms: insights from fossil, biological and molecular data. *Phycologia* 45: 361–402.

SORHANNUS U. 2004. Diatom phylogenetics inferred based on direct optimization nuclear-encoded SSU rRNA sequences. *Cladistics* 20: 487–497.

SORHANNUS U. 2007. A nuclear-encoded small-subunit ribosomal RNA timescale for diatom evolution. *Marine Micropaleontology* 65: 1–12.

STAMATAKIS A., LUDWIG T. & MEIER H. 2005. RAxML-III: a fast program for maximum likelihood-based inference of large phylogenetic trees. *Bioinformatics* 21: 456–463.

SULLIVAN M.J. & CURRIN C.A. 2000. Community structure and functional dynamics of benthic microalgae in salt marshes. In: *Concepts and controversies in tidal marsh ecology* (Ed. by M.P. Weinstein & D.A. Kreeger), Kluwer Academic Publishers, Dordrecht, Germany. pp. 81–106.

SWOFFORD D.L. 2002. *PAUP*: phylogenetic analysis using parsimony (* and other methods)*, ver. 4.0b10. Sinauer Associates, Sunderland, MA, USA.

THOMPSON J.D., GIBSON T.J., PLEWNIAK F., JEANMOUGIN F. & HIGGINS D.G. 1997. The ClustalX windows interface: flexible strategies for multiple sequence alignment aided by quality analysis tools. *Nucleic Acids Research* 24: 4876–4882.

TIFFANY M.A. 2005. Diatom auxospore scales and early stages in diatom frustule morphogenesis: their potential for use in nanotechnology. *Journal of Nanoscience and Nanotechnology* 5: 131–139.

TOYODA K., IDEI M., NAGUMO T. & TANAKA J. 2005. Fine-structure of frustule, perizonium and initial valve of *Achnanthes yaquinensis* McIntire and Reimer (Bacillariophyceae). *European Journal of Phycology* 40: 269–279.

TOYODA K., WILLIAMS D.M., TANAKA J. & NAGUMO T. 2006. Morphological investigations of the frustule, perizonium and initial valves of the freshwater diatom *Achnanthes crenulata* Grunow (Bacillariophyceae). *Phycological Research* 54: 173–182.

TROBAJO R., MANN D.G., CHEPURNOV V.A., CLAVERO E. & COX E.J. 2006. Auxosporulation and size reduction pattern in *Nitzschia fonticola* (Bacillariophyta). *Journal of Phycology* 42: 1353–1372.

UNDERWOOD G.J.C. & KROMKAMP J. 1999. Primary production by phytoplankton and microphytobenthos in estuaries. *Advances in Ecological Research* 29: 93–153.

VAN DE PEER, Y., CAERS A., DE RIJK P. & DE WACHTER R. 1998. Database on the structure of small ribosomal subunit RNA. *Nucleic Acids Research* 26: 179–182.

VAN DE PEER Y., NEEFS J.-M., DE RIJK P. & DE WACHTER R. 1993. Reconstructing evolution from eukaryotic small-ribosomal-subunit RNA sequences: calibration of the molecular clock. *Journal of Molecular Evolution* 37: 221–232.

VAN LANDINGHAM S.L. 1978. *Catalogue of the fossil and recent genera and species of diatoms and their synonyms. Part VII*. Rhoicosphenia *through* Zygoceros. J. Cramer, Vaduz, Liechtenstein.

VON STOSCH H.A. 1962. Über das Perizonium der Diatomeen. *Vorträge aus dem Gesamtgebiet der Botanik* 1: 43–52.

VON STOSCH H.A. 1982. On auxospore envelopes in diatoms. *Bacillaria* 5: 127–156.

VON STOSCH H.A. & KOWALLIK K.V. 1969. Der von Geitler aufgestellte Satz über die Notwendigkeit einer Mitose für jede Schalenbildung von Diatomeen. Beobachtung über die Reichweite und Überlegungen zu seiner zellmechanischen Bedeutung. *Österreichische botanische Zeitschrift* 116: 454–474.

VON STOSCH H.A., THEIL G. & KOWALLIK K.V. 1973. Entwicklungsgeschichtliche Untersuchungen an zentrischen Diatomeen. V. Bau und Lebenszyklus von *Chaetoceros didymum*, mit Beobachtungen über einige andere Arten der Gattung. *Helgoländer wissenschaftliche Meeresuntersuchungen* 25: 384–445.

WITKOWSKI A., LANGE-BERTALOT H. & METZELTIN D. 2000. Diatom flora of marine coasts I. *Iconographia Diatomologica* 7: 1–925.

Received 12 January 2008; accepted 18 February 2008
Associate editor: Wiebe Kooistra